A THESIS SUBMITTED TO
THE GRADUATE SCHOOL OF NATURAL AND APPLIED SCIENCES
OF ÇANKIRI KARATEKİN UNIVERSITY

HUMAN IDENTIFICATION USING PALM PRINT IMAGES BASED ON DEEP LEARNING METHODS AND GRAY WOLF OPTIMIZATION ALGORITHM

IN PARTIAL FULFILLMENT OF THE REQUIREMENTS
FOR
THE DEGREE OF MASTER OF SCIENCE
IN
ELECTRONICS AND COMPUTER ENGINEERING

BY

FIRAS HASAN ALI ALSHAKREE

ÇANKIRI

2022

HUMAN IDENTIFICATION USING PALM PRINT IMAGES BASED ON DEEP LEARNING METHODS AND GRAY WOLF OPTIMIZATION ALGORITHM

By Firas Hasan Ali ALSHAKREE

December 2022

We certify that we have read this thesis and that in our opinion it is fully adequate, in scope and in quality, as a thesis for the degree of Master of Science

Advisor **:** Assist. Prof. Dr. Ayhan AKBAŞ

Examining Committee Members:

Chairman **:** Asst. Prof. Dr. Ayhan AKBAŞ
Computer Engineering
Abdullah Gül University

Member **:** Asst. Prof. Dr. Selim BUYRUKOĞLU
Computer Engineering
Çankırı Karatekin University

Member **:** Asst. Prof. Dr. Cevat REHABİ
Software Engineering
İstanbul Topkapı University

Approved for the Graduate School of Natural and Applied Sciences

Prof. Dr. İbrahim ÇİFTÇİ
Director of Graduate School

I hereby declare that all information in this document has been obtained and presented in accordance with academic rules and ethical conduct. I also declare that, as required by these rules and conduct, I have fully cited and referenced all material and results that are not original to this work.

Firas Hasan Ali ALSHAKREE

ABSTRACT

HUMAN IDENTIFICATION USING PALM PRINT IMAGES BASED ON DEEP LEARNING METHODS AND GRAY WOLF OPTIMIZATION ALGORITHM

Firas Hasan Ali ALSHAKREE

Master of Science in Electronics and Computer Engineering

Advisor: Asst. Prof. Dr. Ayhan AKBAŞ

December 2022

In this thesis, we used palm print images for human identification. This thesis contains four steps. First, the features of the palm print images are extracted by pretrained network that uses the deep learned network. Thre pretrained networks such as Googlenet squesse net and Alexnet are used to extract the features from the images. Then the best features were selected by using the Gray-Wolf optimization method. In the third step, these features are used in the nearest neighborhood method for recognition of the dataset to be used in the test data. Finally, we evaluated the results with recognition rate that calculated the percentage of the recognitions of the mistake index and correct index from the dataset. The aim of this thesis is to use the Gray-Wolf Optimization method and deep learning to get high recognition rate. In this study we used two famous dataset such as Polytechnic Hong Kong university dataset and Tongji Contactless datasets, the recognition rate for the different methods is evaliated and tested. We are showing that the proposed method has a very high performance in the recognition rate than other different methods such as principle component analysis, Local binary pattern and laplacian of gaussian gabor transform. The recognition rate from the proposed method we obtain 96.72.

2022, 55 pages

Keywords: Human identification, Palm print images, Deep learning, Gray Wolf Optimization algorithm**,** Recognition rate

ÖZET

DERİN ÖĞRENME YÖNTEMLERİNE VE GRİ KURT OPTİMİZASYONU ALGORİTMASINA DAYALI PALMİYE BASKI GÖRÜNTÜLERİ KULLANARAK İNSAN TANIMLAMA

Firas Hasan Ali ALSHAKREE
Elektronik ve Bilgisayar Mühendisliği, Yüksek Lisans
Tez Danışmanı: Dr. Öğr. Üyesi Ayhan AKBAŞ
Aralık 2022

Bu tezde insan tanımlaması için avuç içi baskı görüntüleri kullanılmaktadır. Bu tez dört adım içermektedir. İlk adımda, avuç izi görüntüleri üzerinde derin öğrenme ve yerel ikilinin kullanıldığı özellik çıkarım yöntemi kullanılmıştır. Daha sonra Gray-Wolf optimizasyon yöntemi kullanılarak en iyi özellikler seçilmiştir. Üçüncü adımda bu öznitelikler test ve doğrulama verilerinde kullanılacak veri setinin tanınması için en yakın komşuluk yönteminde kullanılmıştır. Son olarak, veri setinden hata indeksi ve doğru indeksin tanınma yüzdesini hesaplayan tanıma oranı ile sonuçlar değerlendirilmiştir. Bu tezin amacı, yüksek tanıma oranı elde etmek için Gri Kurt Optimizasyonu yöntemini ve derin öğrenmeyi kullanmaktır. Bu çalışmada Polytechnic Hong Kong üniversitesi veri seti ve Tongji Contactless veri seti gibi iki ünlü veri seti kullandık, farklı yöntemlerin tanınma oranı değerlendirildi ve test edildi. Önerilen yöntemin tanıma oranında ilke bileşen analizi, gradianet histogramı gibi diğer yöntemlere göre yüksek performansa sahip olduğunu gösterdik. Elde ettiğimiz önerilen yöntem için tanıma oranı 96,72 çıkmıştır.

2022, 55 sayfa

Anahtar Kelimeler: İnsan tanımlama, Palm print resimleri, Derin öğrenme, Gri Kurt Optimizasyon algoritması, Tanıma oranı

PREFACE AND ACKNOWLEDGEMENTS

I would like to thank my thesis advisor, Asst. Prof. Dr. Ayhan AKBAŞ, for his patience, guidance and understanding.

Firas Hasan Ali ALSHAKREE

Çankırı-2022

CONTENTS

LIST OF ABBREVIATIONS

ACO	Ant colony optimization
ANN	Artificial neural network
CNN	Convolutional neural network
DL	Deep learning
DNN	Deep neural network
GA	Genetic algorithm
GWO	Gray wolf optimization
ID	Image denoising
LBP	Local binary pattern
LoG	Log-Gabor
PCA	Principal component analysis
PSO	Particle swarm optimizations
ROI	Region of interest

LIST OF FIGURES

LIST OF TABLES

1. INTRODUCTION

1.1 Background

Nowadays, there is a lot of interest in biometric identification, particularly with the development of internet technology and digital computing. New security issues were raised by the high popularity of the internet, which raised the number of network users. More dependable techniques must be employed to protect user data on public networks like the internet as security issues reach a new stage. There is a lot of interest in the new biometric recognition, particularly with the development of internet technology and digital computing. New security issues were sparked by the rise in network users caused by the popularity of the internet. More dependable techniques need to be employed to protect users' data on open networks, including the internet, as security problems enter a new stage. Traditional personal authentication in cyberspace needs to be improved because of new kinds of digital life like the internet banking and e-commerce (Balasubramanian 2016).Online banking and e-commerce compelled engineers to improve the way of personal identification in cyberspace (Adhinagara et al. 2011).

In the early stages of personal verification, passwords and other straight forward user credentials were used to protect internet-based services like e-commerce and internet banking. It is also being improved upon in order to increase its dependability and stop computers other than the one in question from accessing the service by employing a digital certificate, such as a digital signature (Winn 2022). Some samples of the palm print images that are shown in Figure 1.1.

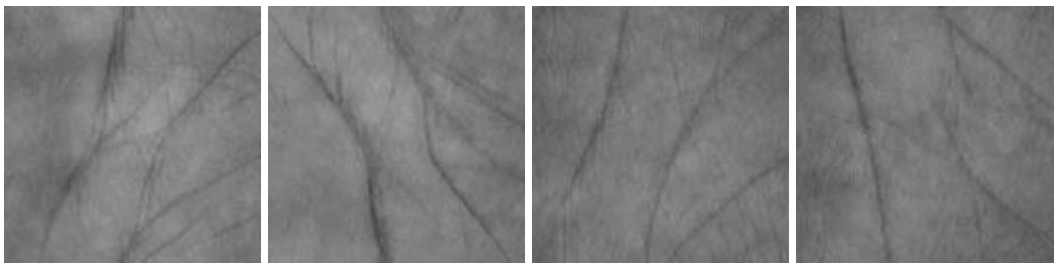

Figure 1.1 Some palm print images

As internet technology has developed, a sizable number of people have participated in networks where a sizable amount of data has been transferred over those networks. It is necessary to safeguard the data supplied across the internet and other web networks against any hostile attacks, such as hacking (Adhinagara et al. 2011).

The user identification number (ID) and password assigned to each candidate are private and particular, and they must be entered together while registering for the network. Such a technique could stop unauthorized individuals from accessing the data storage via the secured server. This technique is deployable on both the internet and intranet networks and may be utilized in online applications as well as other software applications (Matheswaran et al. 2021).

As networks become more complex and software technology advances, password protection alone is no longer sufficient to protect private information from unauthorized access. Secure networking is one of the new methods for enforcing security that have evolved. Virtual networking technology has been viewed as an additional benefit for public networks. several virtual private networks can be set up inside the larger network using software-based networking. Over a larger network, each virtual private network may be utilized to secure specific individuals (Raut et al. 2017).

The leased line technology offered by the internet service providers allows a large number of internet users to be connected to one another. If sensitive information is exchanged across that link, such as during financial transactions, between two parties, it should be protected against unwanted access. To create a virtual tunnel and secure the communication between those parties, a virtual private network might be employed (Venkateswaran 2001).

The key to the security procedure, according to the author, is identifying the people engaged in any transaction across any sort of network. In other words, if the person is correctly identified, there won't be any more illegal access to the system. This innovation could spare the network the expense of investing in new security measures. In other words, instead of protecting networks to make them less vulnerable to unauthorized

access, create a new user (candidate) identification to prevent the replication of the candidate themselves (Sato et al. 2013).

More security issues have arisen as a result of the advancement of digital computing technologies and the rapid increase in data sharing through the internet and web portals, making password credentials and digital signatures unreliable. The use of biometric recognition technologies has significantly improved how complicated web networks are secured. However, biometrical recognition uses traits like the person's face, fingers, eyes, speech, etc. to identify them and then grant them access (Sato et al. 2013).

One of the crucial biometric identification methods that is utilized for personal identification and incorporates a multitude of crucial elements is palm recognition. After preprocessing, we can use the palm image in the features extraction procedure. The size and color of the palm have been utilized as distinguishing characteristics to identify the hand palm. The performance of biometrical identification systems has significantly changed thanks to advances in data technology, machine learning, and deep learning, which have increased recognition accuracy and cut down on the time it takes the system to identify an image.

1.2 Problem Statement

Various studies on personal identification employing methods like passwords, credentials, fingerprints, facial recognition, speech identification, etc. are discussed in the literature. The current technologies, though, are aware of the flowing issues.

(A) To safeguard user data from harmful assaults and eavesdropping, many web portals still employ the old technique of personal identification by passwords and credentials. Password protection is no longer effective owing to password guessability with the development of digital technologies. Finaly saying that, we can not use a single password to secure the privacy of such important information, like banking information.

(B) As an alternative, some businesses have created digital signatures that function as a virtual private network, keeping only the people involved connected while preventing outside influence. Such digital certificates could be downloaded and installed on the candidate computer via the web portal (for example, a bank web system). The issue is that a digital certificate can be downloaded by anyone, making it useless for protecting personal information.

(C) There are numerous methods for incorporating the so-called biometric traits of an individual into personal identification, where an individual (user/candidate) must be physically present to access any protected service. In terms of data consistency, these methods have also encountered significant difficulties. Human palprint characteristics cannot stay the same throughout life; they are therefore more sensitive to the effects of aging. The system's database can be regularly upgraded to address this issue. The cost of updating data will be high for large recognition systems, particularly those that include many thousands of candidates, because all features and preprocessing must be redone in accordance with the new database. On the other hand, the so-called has a significant impact on human palmprint recognition systems.

(D) On the other hand, the so-called occluding features have a significant impact on human palmprint recognition systems. If the user or applicant changes his or her appearance by donning a mask, growing a beard, using makeup, etc., palmprint recognition may become very difficult. In such cases, the palmprint recognition system will be useless because the characteristics of the testing stage and the training stage are drastically different.

(E) As evidenced in the literature, machine learning techniques have been incorporated with numerous personal identification systems to improve recognition accuracy. Accuracy levels, however, continue to be debated and require improvement. Additionally, practical metrics for performance measurement have been seen in numerous earlier investigations. A thorough examination of system performance might necessitate looking at many performance indicators.

1.3 Research Objectives

A unique biometrical recognition method is suggested employing hand palm features to address the issues described in the preceding section. The hand palm is recognized as a source of important biometrical characteristics that are resistant to the effects of aging. There are several traits on the hand palm that are independent of age or other factors like hair growth. The enumerated system must be implemented for the following conditions to be met.

a) the creation of a hand palm based personal recognition system that can record hand features and use them to identify characters.

b) the adoption of features that are permanent and have no internal or external effects in the recognition process. The selected features in this study are tested and the relible feature are signed.

c) to remove the noise of the palm print images that effected by the imaging system from device can be removed by convolving of the filter. This issue was solved by implementing the convolutional neural network.

d) using the convolutional neural network for feature extraction we can enhance the features number and find all features that affect the recognition rate.

e) evaluating performance of the suggested method using a recognition rate that obtaine from the test data.

1.4 Motivation of Study

The essential motivation of this study is using the convolutional nural network based on three famus pretrained network to extract the features from the palm print images and reduce the feature number of these features based on the metaheuristic method. In this

study gray wolf optimization and other methods such as the Ant colony optimization (ACO) method and genetic algorithm (GA) and particle swarm optimizations (PSO) are used and tested.

1.5 Advantage of Study

The main advantage of the study can be summed up as in the following steps:

a) Get high accuracy for the recognition rate
b) Use the best features that effect on the recognition rate
c) Use different robust method and obtain the accurate results

1.6 Disadvantage of Study

a) The implementation of the method needs more time to extract the features.
b) The data that used in this study are contains only 500 person images.
c) The pretrained network is used to extract the features

1.7 Aim of Thesis

The aim of this thesis is the use the pretrained network and use the gray wolf optimization to get high accuracy and obtain the best features that can obtain the high performance on recognition rate.

1.8 Thesis Structure

The five technical chapters that make up this thesis report's methodologies and findings each focus on one of the study's various approaches. The first chapter of the thesis, named "introduction," contains a brief introduction to the biometric recognition approach and its necessity in enforcing data security. Also, chapter one contains a list of the issue statement and the study materials. These following chapters are: Chapter 2, "Literature

review," Chapter 3, "Material and methods," and Chapter 4, "results and discussion." The past research studies undertaken in the same field as this thesis are described in detail in Chapter 2. The theoretical portion of this thesis, database setup, feature extraction, and feature selection, is covered in length in Chapter 3. The empirical steps taken to put the ideas and suggested approach into practice, together with the findings and outcomes of this study, are covered in chapter 4. The conclusion and a list of the sources utilized to support this work are found in the final part of the thesis.

2. LITERATURE REVIEW

2.1 Palmprint Recognition

A crucial step in any security system, self-recognition of personal verification requires that an approved accessor has the same capabilities as any other accessor who is ready to log in. According to a study, biometric features should be used in place of traditional identity checks like passwords and credentials (Yang et al. 2021). Figure 2.1 depicts a demonstration of biometric features that could take the role of text password protection.

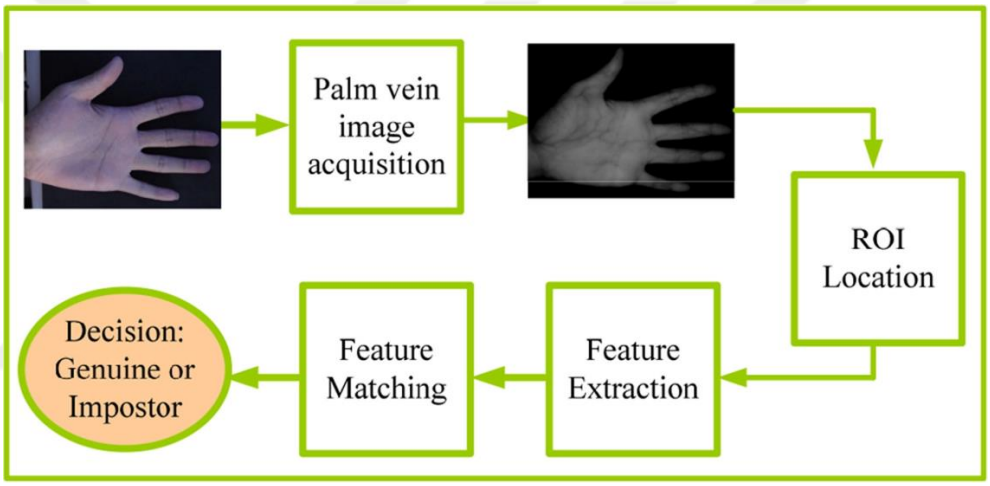

Figure 2.1 An example of palmprint features that could take the place of text password protection (Wu et al. 2020)

According to Nguyen et al. (2015), finger impressions may serve as a reliable method of identification in cases where a candidate may be identified by certain characteristics of his or her fingers. The research has been broadened to encompass various sources of biometrical traits other than the palmprint images. Like the thumb, each person's fingers are made up of indelible lines and circles. The system can accept these features from the fingers, which are similarly subjected involves feature extraction and preprocessing in order to distinguish the important characteristics (Azman et al. 2019).

Even in ancient times, humans used to recognize each other through speech, as well as enemies and wild animals through their voices. To put it another way, audible signals are critical for identifying the candidate. More specifically, Jiaqiang et al. (2013) demonstrated that speaker identification algorithms for personal verification processes can utilise human speech. The speech signal is also brimming with important characteristics and traits that can be utilized to identify users. For the aime of isolating the speech features, the speaker recognition system performs digital signal processing at increased computing costs (Nguyen et al. 2008).

The five steps shown in Figure 2.2 that make up a traditional palmprint identification procedure are palmprint picture acquisition, database, preprocessing, feature extraction, and matching.

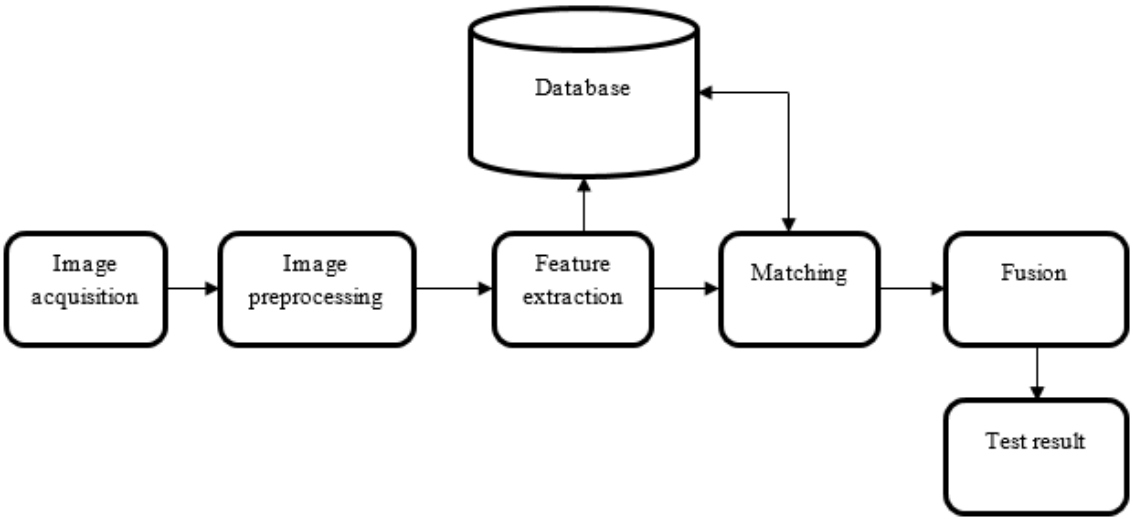

Figure 2.2 The system's flow-process diagram for recognizing palm prints (Zhong et al. 2019)

The palmprint pictures are captured by the acquisition device in a variety of ways that are consistent with later recognition. The core of the preprocessing stage is the region of interest (ROI). The reference coordinate system approach, which is shown in Figure 2.3, is one of the often-employed methods.

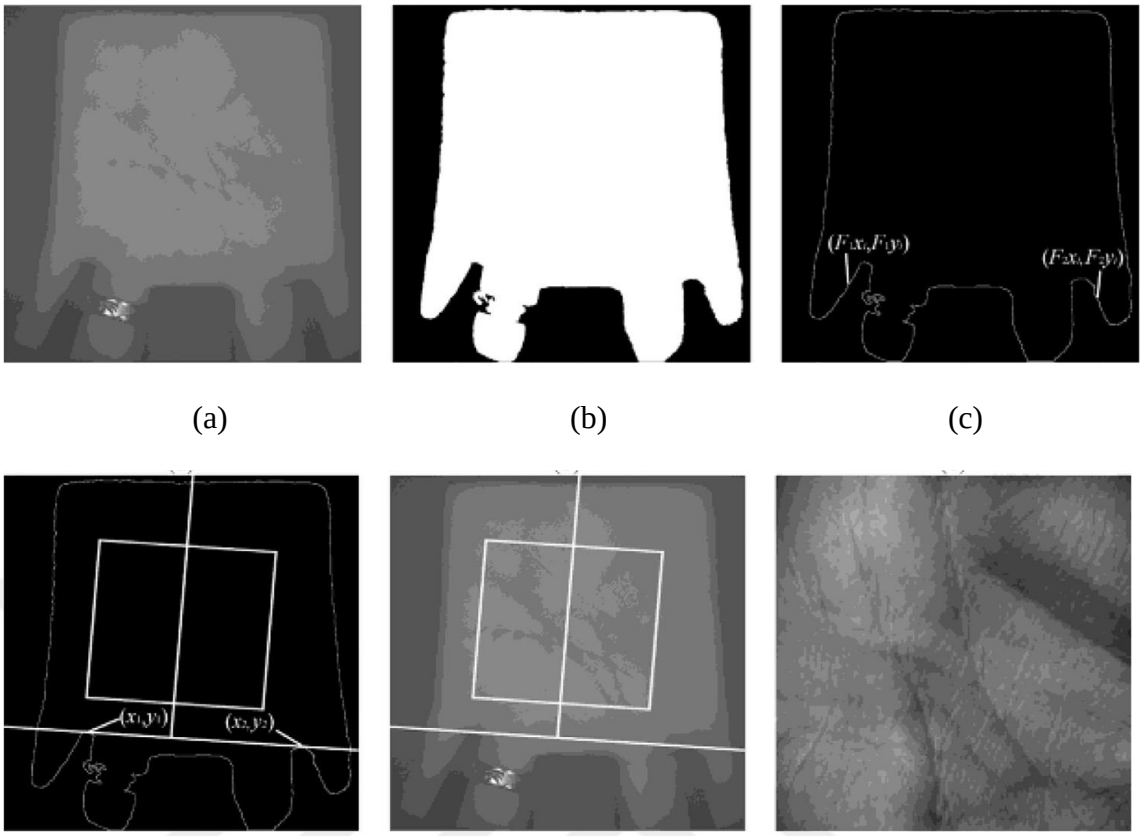

Figure 2.3 (a) the original image, (b) the binary image, (c) border tracking, (d) setting up a coordinate system, (e) extracting the central region, (f) obtaining a ROI sample (Guo et al. 2012)

The feature extraction was taken into account when a variety of algorithms, that includes subspace methods, learning methods, line-based and coding-based ways of approaching were presented (Zhang et al. 2012). Each method takes information from a local or global perspective and can have its distinctive advantages. The matching procedure compares testing samples to other samples in the database using a given matcher.

2.2 Image Acquisition

Each of the acquisition algorithms is founded on a particular database and a certain application orientation. Because of the changes in the real world, lots of effective algorithms recommended in the ideal acquisition condition aren't considered as

applicable for the actual application of palmprint recognition. As a result, it is crucial to build up various databases to replicate various situations and check whether a specific technique works in the research setting. After that, adjustments can be made to get a better experimental outcome. Numerous new databases have been created in the last ten years, with examples found in (Bingöl and Ekinci 2017, Zhang et al. 2017, Chaa et al. 2017, Veigas and Kumari 2022). A lot of databases are being created using modern devices that capture images on various platforms, except for some that use classic cameras and classic acquisition methods, such as CCD-based (charge-coupled device) scanners, digital cameras, and video camerasin order to collect palmprint images (Zhang and Gu 2013, Jia et al. 2021). For instance, Aykut and Ekinci (2013) achieved online palm image acquisition, using a CCD camera, a hand positioning platform, a DC auto iris lens, and uniform LED (light emitting diode) light sources. The most often used data across all image formats is 2D palmprint data since it is both easily available and manageable. Numerous databases also contain information on different types of palmprints, including 3D (Ni et al. 2015, Yang et al. 2013, Zhao et al. 2022), multispectral (Xu et al. 2012), and minute (Dai and Zhou 2010). With the establishment of around 25 new palmprint databases, there are now 4,200 samplers in total. To imitate genuine and various situations, which is a fundamental requirement in the process of obtaining images, is sufficient.

2.3 Preprocessing

The 1st stage in feature extraction and matching is preprocessing. The results of recognition are significantly influenced by the caliber of preprocessing. We primarily concentrate on the creation of algorithms to extract ROI. Because, in contrast to other processes like image enhancement, image filtering, and the rest, it is the primary step in the preprocessing stage. Distance can be the most significant measurement objective in ROI extraction in the last ten years. The connection line between the valley points and the edge of the ROI is maintained by this method at a constant pixel distance (Wang et al. 2008, Meraoumia et al. 2011, Yue et al. 2009, Attia et al. 2022). In other words, if researchers just employ the distance principle due to the size variation of palmprint photos, valuable region for feature extraction will not be extracted accurately. As a result,

the outcome of recognition falls short of the high bar. As a result, alternative metrics like ratio (Hammami et al. 2014) and angle (Badrinath and Gupta 2012, Tiwari et al. 2013, Attia et al. 2022) are now commonly used.

In this thesis, the preprocessing concept are solved by using the convolutional neural network. That's mean we dont need to use the preprocessing methods to reduce the noise of images, and the CNN that used in this study use the convolutional layers as mask to filter the images. In convolutional neural network the features of the images are extracted with the denoised form. Actually, the convolutional neural network uses the filter mask and many layer of convolving of the matrix on the image to extract the vector matrix. The advantage of this method that we used in this study is that we dont need to use the preprocessing stages and directly we can use the CNN to implement on the image and extract the features from the images.

In next chapter we will show the method that we use on the images. As well as the extarcted features from convolutional neural network has a big number, and this issue can not help us to recognise the persons. Because the huge number of features can be disturbe the recognition system and the system can not give us correct results. For this reason, we should use some method to lessen the number of features. In this study the geray wolf optimization method is used to reduce the feature number. Gray wolf optimization method is robust method to select the features. Becuase this method has fast convergence process time and is flixable to find the nearest neighbor of the features.

3. MATERIALS AND METHODS

3.1 Background

In this part the material and methods that are used to palm print recognition are presented. First of all, the convolutional neural network with trained newrok is introduced. Then the gray wolf optimization method is explained. The gray wolf has high performance than other metaheuristic method to find the best cluster of thefeatures. Finally, the recognition step that include the nearest neighboor value will explained. For nearest neighboor method we used the Euclidan distance method. In this method the distance between test feature and train features are calculate and save in the vector. And then the minimum distance of vector calculates. After that the index will be the result of the recognition person.

3.2 Summary of the Study

The summary of the given method for the palm print recognition system that used in this thesis is shown in Figure 3.1. All steps of this flowchart will be explained in next sections. In this work the Matlab software with 2022a version is used to implement the proposed method. Also, the Ram of 4GHz, Core i7, Intell, Asus is used. The major contribution of this thesis is the use of the convolutional neural network with different pretrained network such as google net and squees net, and also use the gray wolf optimization algorithm to find the accurate features from the CNN features. Also show the fast method such as Euclidian distance method to recognize the palm print images.

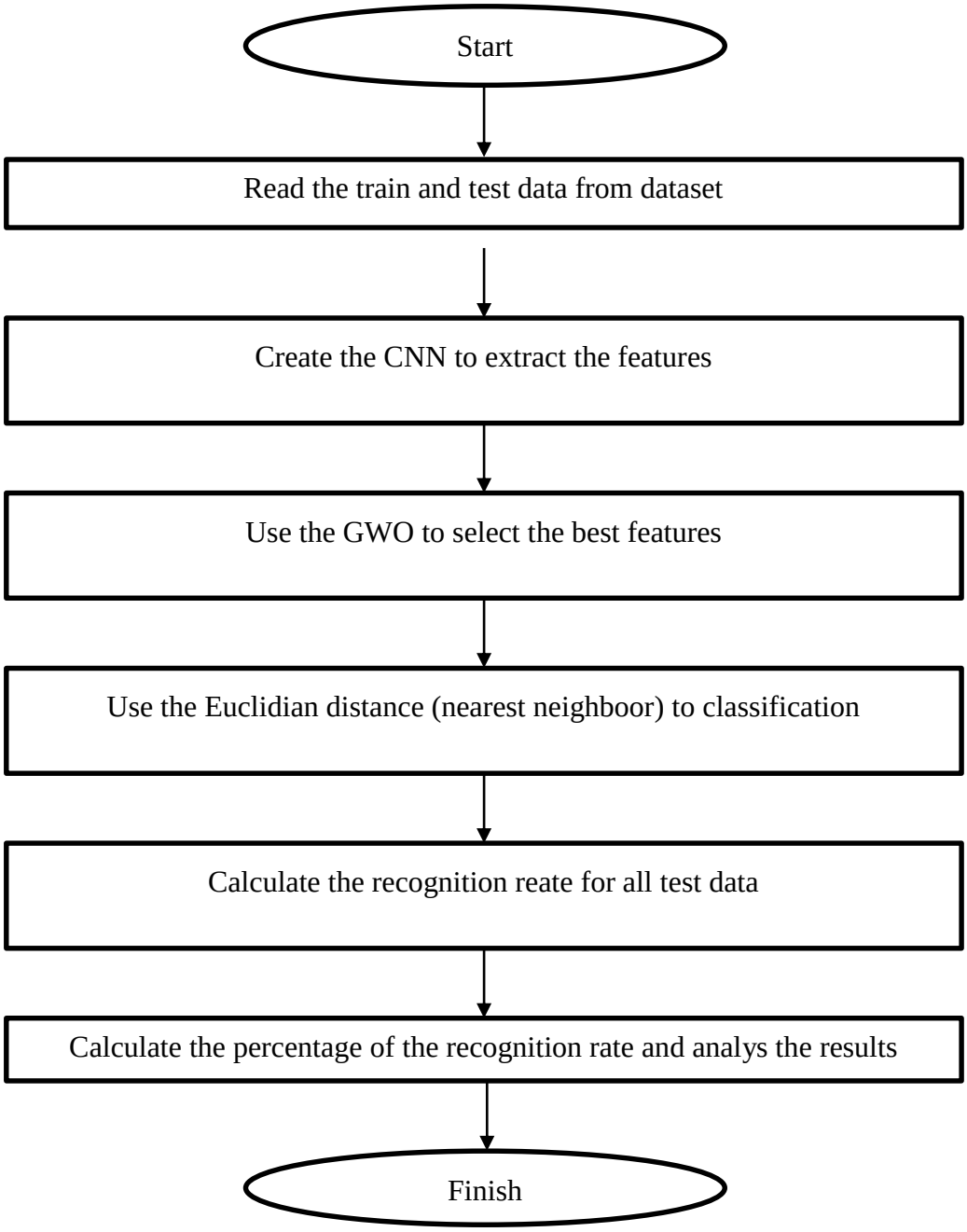

Figure 3.1 Flowchart of overall system

3.3 Convolutional Neural Network

In this section the convolutional neural network is presented to feature extraction of the images from the palm print image dataset. Convolutional neural network recently used in image recognition systems.

The NN numerically represents the NNs in an individual's cerebrum, that are made up of a big number of linked neurons and nerve cells. Through transient motivations of the electrical impulses produced by a layer of cells, that are referred to as cells, neurons are matched up. This information is transmitted as electrochemical correspondences, or neurotransmitters, from one neuron to the next. These intersections are found on branches that connect them to the cell body, or dendrites, which carry signals from a lot of neurons to the body of the nerve cell. In the body of the nerve cell, qualities are processed with the goal of choosing the neuron's outcome, whether or not to produce an electrical sign, also referred to as a signal. A signal that is transmitted from one neuron to the next may have either an excitatory or an inhibitory effect on the receiving cell. While the excitatory influence makes the getting neuron fire, the inhibitory effect stops the neuron from terminating. Nevertheless, the influence of different information sources is constrained by the conductivity of the electrochemical junctions that carry those information sources into the cell body (Fernández-Montoya et al. 2018, Turčaník and Javurek 2016, Turčaník 2017, Abdoun et al. 2018, Srivastava et al. 2014, Kingma and Ba 2014, Glorot and Bengio 2010, Krizhevsky et al. 2017, Shin et al. 2016, Szegedy et al. 2016).

The final layer's output, which may be a channel or a maximum pooling layer, is totally leveled to a single vector and connected to the FFNN. The neurons in the completely linked layers are now able to discern sophisticated two-layered neighborhood highlights in the data due to the various channel mixtures in the layers. Additionally, a three-layered contribution to NN that separates the data into layers of two-layered exhibits can be handled. The NN develops numerous channel layouts for each layer after that, and more advanced levels can blend highlights from multiple layers (Konda 2016). In tasks where distinct choices are made using varying load values among their neurons, two indistinguishable NNs could be used (Sethi and Jain 2014, Hecht-Nielsen, 1992, Miikkulainen et al. 2019, Schmidhuber 2015, Torrey and Shavlik 2010, Tan et al. 2018, Ravishankar et al. 2016, Yin et al. 2019, Gopalakrishnan et al. 2017, Yu et al. 2017).

In this study three famus pretrained networks are used to feature extractions. These networks are: Squeeznet, Alexnet and Googlenet. These pretrained networks have huge layer of neurones adn contain 68, 168, 177 layers respectively. These networksa were

trained for object recognition, texture, palmprint recognition, etc. Also, the results shos that the use of these networks has high performance to find the features and also has high performance in trecognition rate of the palmprint image dataset.

In the later part, the gray wolf optimization is presented to use in the features matrix to select the best features.

3.4 Pretrained networks

In this thesis, the pretrained networks have been used to extract the features from the palm print images.

3.4.1. Googlenet

The goal of GoogLeNet is to increase both the learning capacity and the effectiveness of the CNN parameters. Sparse connections were used by GoogLeNet to solve the issue of redundant data. It reduced costs by skipping over unnecessary channels. The intercepting module, which concatenates feature maps produced by various filter sizes, was made available by GoogLeNet (Xin et al. 2015).

In this thesis, the GoogleNet with 144 layers is used as a pretrained network to extract the features from the leukemia images that are benign and malignant. 1024 features are selected for each image to train. As seen this number is a huge number for training machine learning, and sometimes the classifier has a mistake to find the target.

3.4.2. AlexNet

The AlexNet architecture contains 5 convolutional layers, three max-pooling layers, 2 normalization layers, 2 fully connected layers, and 1 softmax layer. Nonlinear activation function ReLU and convolutional filters make up every convolutional layer (Alom et al. 2018).

3.4.3. SqueesNet

SqueezeNet is a convolutional neural network that is consisted of 18 layers. A pretrained version of the network that has been trained on over than a million images is present in the ImageNet database. A number of animals, computer parts, and a pen are between the 1000 different object categories that the pretrained network can classify images into (Koonce 2021).

3.5 Gray Wolf Optimization

The GWO imitates the directorial hierarchies and also the hunting mechanisms that gray wolves exhibit in their own environment, essentially. Each pack is made up of alpha, beta, delta, and omega grey wolves. In addition, there are three steps in their hunting procedure: scouting, encircling, and attacking prey. All these procedures are carried out concurrently with the optimization operation. GWO, a new and effective meta-heuristic technique, is offered by Mirjalili (Mirjalili et al. 2014). Since it is based on animals and nature, it is comprehended and practical to execute. The primary advantage of GWO is its adaptability, simplicity, and clarity. When compared to other well-known and effective meta-heuristic conceptions, a few recent research indicates that GWO may offer gratifying outcomes. For instance, this occurred when Mirjalili used 29 test functions in order to compare GWO with the Gravitational Search Algorithm (GSA), Differential Evolution (DE), PSO, Evolution Strategy, and Evolutionary Programming. Figure 3.2 depicts the gray wolf's hierarchies.

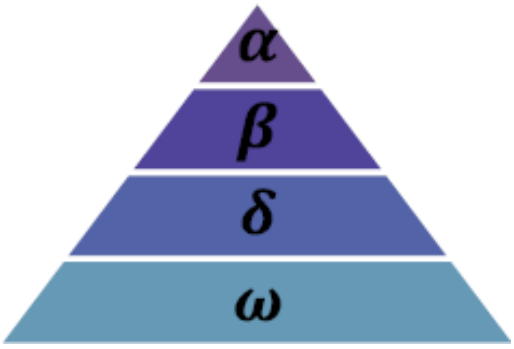

Figure 3.2 Hierarchies of the gray wolf

Any optimization problem that postulates the best solution, or alpha (α), can be solved mathematically by illustrating the wolf's social hierarchy. The expressions "beta" (β) and "delta" (δ) refer to the second- and third-best solutions, respectively, while "omega" (ω) refers to other options.

In teaching and the explaining of the gray wolf algorithm, we can notice that this algorithm is formed of 3 main steps:

1- Track, search, chase, and approach the potential prey.

2- Harass and encircle a prey until the prey no longer moves.

3- Attack the prey.

It can access any location among the points because of the accidental vectors $\overrightarrow{r_1}$ and,$\overrightarrow{r_2}$ as Figure 3.2 illustrates. Consequently, a gray wolf may update its location in any random location in the space surrounding the prey using Equations 1 and 2.

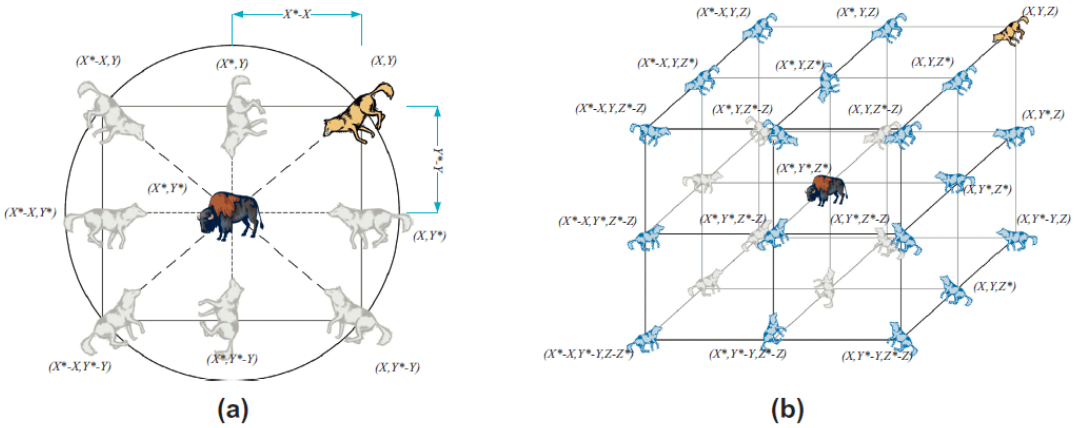

Figure 3.3 Gray wolf's structures to get prey

The attack is commanded by the alpha wolf as the prey is surrounded by wolves and do not move anymore. The reduction of the vector an is used to model this process. The coefficient vector A reduces as (a) lowers since it is an accidental vector in the range [-2a, 2a]. The wolf alpha will approach the prey (and the other wolves) if |A|<1, and the

wolf will avoid the prey (and the rest of the wolves) if |A|> 1. All wolves must update their positions in accordance with the positions of the alpha, beta, and delta wolves according to the gray wolf algorithm.

During the hunt, gray wolves surround the predation. The equations that follow provide a mathematical representation of the siege behavior. In the relations shown below the current iteration t, A, and C are coefficient vectors, Xp is the prey position vector and X is the position vector of the gray wolf (see Equation (3.1) and (3.2)).

$$\vec{D} = \left|\vec{C}.\vec{X}_p(t) - \vec{X}_n(t)\right| \quad (3.1)$$

$$\vec{X}_n(t+1) = \vec{X}_p(t) - \vec{A}.\vec{D} \quad (3.2)$$

Vectors A and C are calculated as in Equations (3.3) and (3.4):

$$\vec{A} = 2\vec{a}.\vec{r}_1 - \vec{a} \quad (3.3)$$

$$\vec{C} = 2\vec{r}_2 \quad (3.4)$$

Here, r_1 and r_2 are the accidental vectors [0, 1] and after iterations, $\vec{a}$ components have been linearly reduced from 2 to 0.

Searching and excavation operations will be typically directed by alpha. Beta and delta wolves may also take part in hunting occasionally. In the mathematical model referring to grey wolf looking behavior, we hypothesized that alpha, beta and delta contain better know-how of prey capacity positions. The three primary answers are excellently stored and the opposite agent must replace their positions in keeping with the position of the nice seek agents in line with the Equations (3.5), (3.6), and (3.7).

$$\vec{D}_\alpha = \left|\vec{C}_1.\vec{X}_\alpha - \vec{X}\right|, \vec{D}_\beta = \left|\vec{C}_2.\vec{X}_\beta - \vec{X}\right|, \vec{D}_\delta = \left|\vec{C}_3.\vec{X}_\delta - \vec{X}\right| \quad (3.5)$$

$$\vec{X}_1 = \vec{X}_\alpha - \vec{A}_1.(\vec{D}_\alpha), \vec{X}_2 = \vec{X}_\beta - \vec{A}_2.(\vec{D}_\beta), \vec{X}_3 = \vec{X}_\delta - \vec{A}_3.(\vec{D}_\delta) \quad (3.6)$$

$$\vec{X}_n(t+1) = \frac{\vec{X}_1 + \vec{X}_2 + \vec{X}_3}{3} \quad (3.7)$$

The search steps are shown in Figure 3.3.

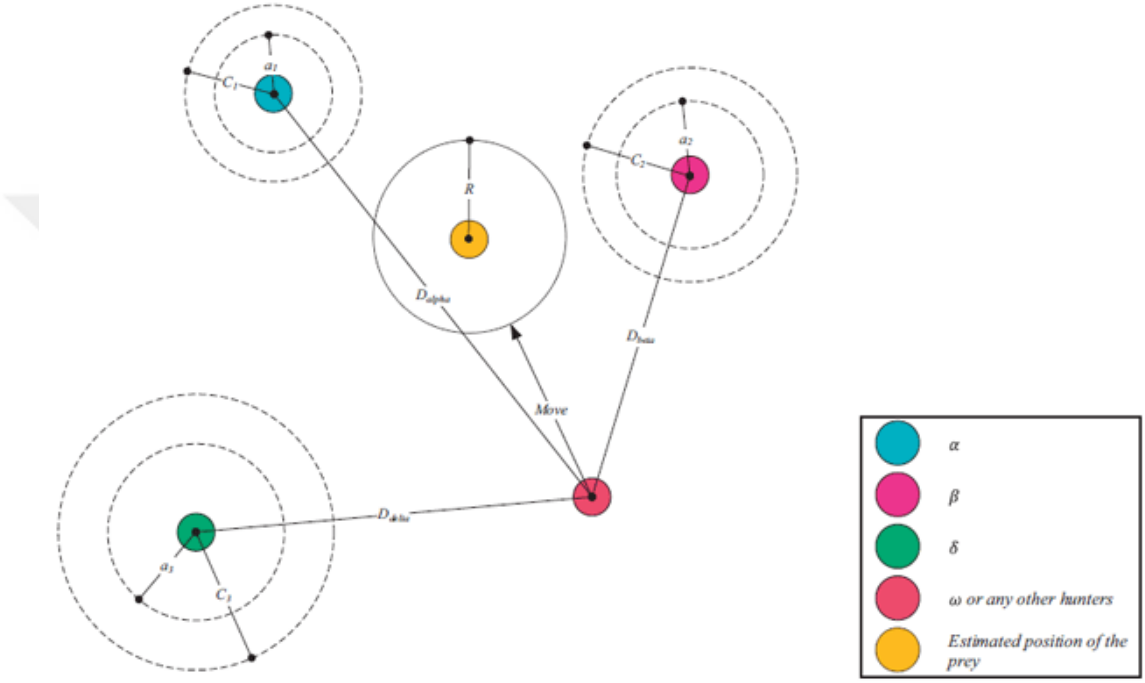

Figure 3.4 Search steps

Based on to the details of the flowchart, the gray wolf algorithm might be considered as the follow. This flowchart can only work by determining the values of vectors A and C. To explain this flowchart is uncomplicated by studying the abovementioned steps. Figure 3.4 indicated the Flowchart of the Gray Wolf Algorithm.

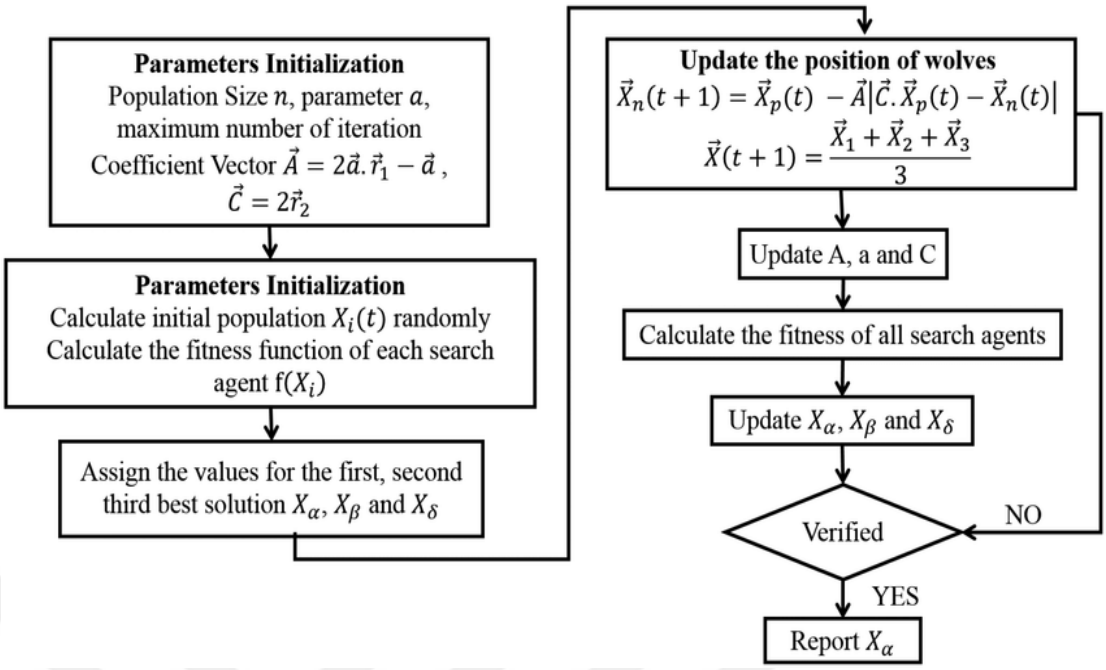

Figure 3.5 Flowchart of Gray Wolf Algorithm

This looks at introduces the grey wolf optimizer into a unique set of rules to generate the global seek vector for decreasing the characteristic numbers from the fault indicatores that created by guide enforcing in Simulink to attain the capabilities for global exploration. Numerous steps are contained in the gray wolf optimizer:

(1) Social hierarchy mechanism

According to their fitness values, the wolves are separated into 4 groups (W1, W2, W3, and W4). The first three groups have the ability to control the wolves and are made up of excellent adaptable gray wolves.

(2) Surround the prey

The grey wolves must surround their prey while predating. A mathematical model can be found in Equations (3.8) and (3.9):

$$\vec{S} = \left|\vec{Q_2} \times \vec{Z_P}(x) - \vec{Z}(x)\right| \tag{3.8}$$

$$\vec{Z}(x+1) = \vec{Z_P}(x) - \vec{Q_1} \times \vec{S} \tag{3.9}$$

In which x represents the cutting-edge new release number. $\vec{S}$ is the distance and route of the wolf from its prey. $\vec{Z_P}$ is the location of the prey. $\vec{Z}$ gives the placement of the wolves. $\vec{Q_1}$ and $\vec{Q_2}$ are coefficient vectors and can be described as in Equations (3.10) and (3.11):

$$\vec{Q_1} = a(2 \times rand(0,\ 1) - 1) \tag{3.10}$$

$$\vec{Q_2} = 2 \times rand(0,\ 1) \tag{3.11}$$

In this equation a is a factor of attenuation. When the range of iterations rises, the coefficient experiences a linear decrease from 2 to zero.

(3) Hunting

The wolf W1 instructs wolves W2 and W3 to reduce the prey's surrounding circle (domain) in order to gain the motive for hunting. The mathematical model is given as in Equations (3.12) and (3.13):

$$\begin{cases} and\vec{S_{W_1}} = \left|\vec{Q_2} \times \vec{Z_{W_1}}(x) - \vec{Z}(x)\right| \\ and\vec{S_{W_2}} = \left|\vec{Q_2} \times \vec{Z_{W_2}}(x) - \vec{Z}(x)\right| \\ and\vec{S_{W_3}} = \left|\vec{Q_2} \times \vec{Z_{W_3}}(x) - \vec{Z}(x)\right| \end{cases} \tag{3.12}$$

$$\begin{cases} and\vec{Z_1} = \vec{Z_{W_1}} - \vec{Q_1} \times \vec{S_{W_1}} \\ and\vec{Z_2} = \vec{Z_{W_2}} - \vec{Q_1} \times \vec{S_{W_2}} \\ and\vec{Z_3} = \vec{Z_{W_3}} - \vec{Q_1} \times \vec{S_{W_3}} \end{cases} \tag{3.13}$$

Where, $\vec{Z}_{W_1}$ $\vec{Z}_{W_2}$, $\vec{Z}_{W_3}$ indicate the positions of wolf W_1, wolf W_2 and wolf W_3, respectively. $\vec{Z}$ gives the location and position information belonging to the remaining wolves. $\vec{S}_{W_1}$, $\vec{S}_{W_2}$, $\vec{S}_{W_3}$ indicate the rout and step size (step length) of wolf W_4 which moves toward wolf W_1, wolf W_2 and wolf W_3, respectively.

(4) Generation a global search vector

The global search vector is defined as the Equation (3.14):

$$\vec{V} = \vec{V} + rand \times (Z_1 + Z_2 + Z_3 - 3P_P(x)) \tag{3.14}$$

The improved position update formula is as in Equation (3.15):

$$P_p(\vec{x} + 1) = \frac{\vec{P_p}(x) + P_p(\vec{x+1}) + \vec{V}}{3} \tag{3.15}$$

In Equation (3.15) the features from the created data matrix can be obtained. These features will be used in the training and testing data.

The flow map of the optimal feature selection of the palm print images using GWO algorithm that is shown in Figure 3.6.

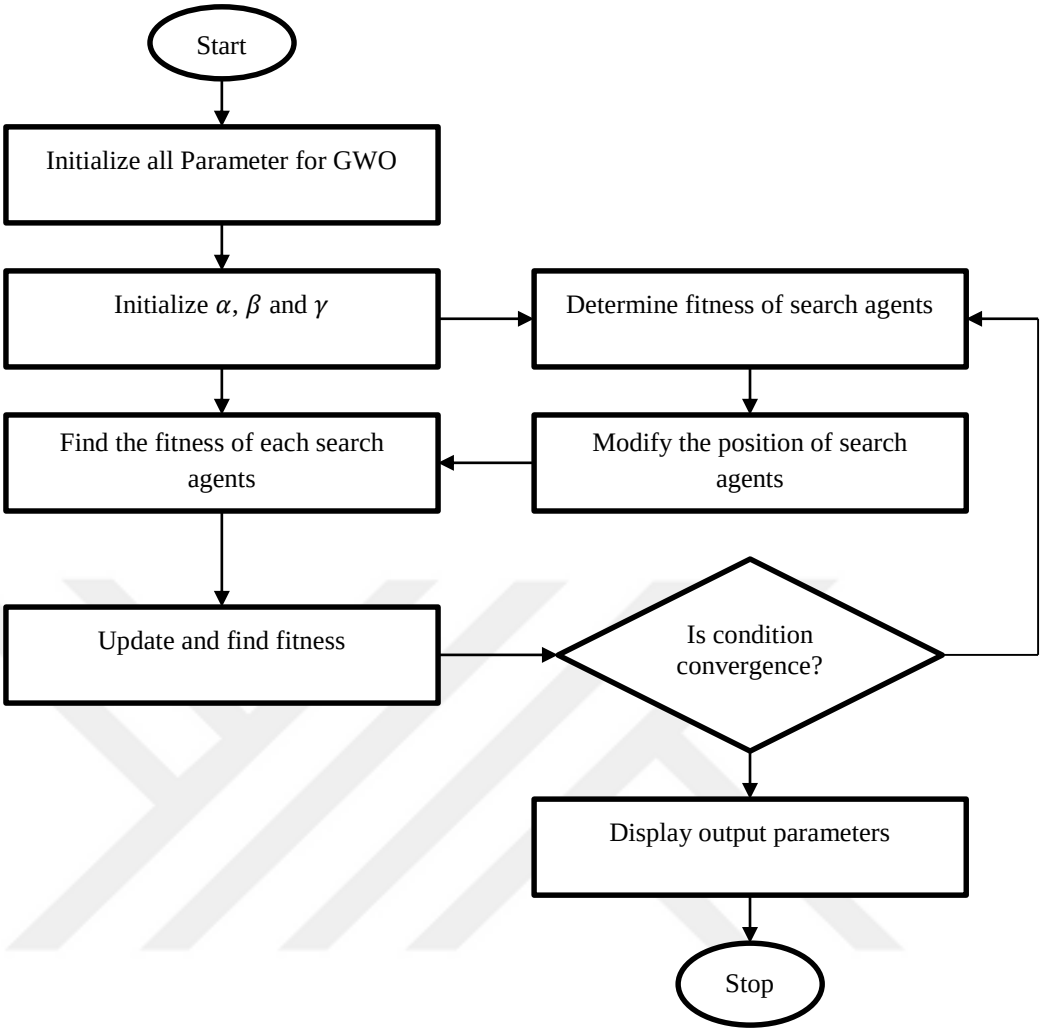

Figure 3.6 Flow chart for grey wolf optimization

After getting the features from the train data and test data, the classifier be used. In this thesis the Euclidian distance classifier that use the nearest neighboor methodology is recommended. Each test image features separately select and then the distance between test image features and all trained features are calculated. The minimum value for this distance is checked and this minimum value index is used as the found image. In next section the Euclidian distance with its formulation is presented.

3.6 Euclidian Distance for Recognition

In this section the Euclidian distance that use the nearest neighboor concept is presented. The Euclidian distance formula is shown in Equation (3.16). In this equation the $Dis(i)$ represent the distance value of the test data and train data, Te_i represent the test vector, Tr_j represent the jth train data.

$$Dis(i) = \sqrt{(Te_i - Tr_j)^2} \tag{3.16}$$

Suppose we have 10 feature number for each person and five test image and 20 train images. One by one we will calculate the test feature vector from all 20 train images, and we save these results in the Dis vector. After that we will find the minimum of them. The minimum of these values will give us the recognized person. This scenario is shown in following Matlab code:

```
FeatureTest = FeaturesTest1(K,:);
Euc_dist = [];
for Tn = 1:size(FeaturesTrain1,1)
FeatureTrain = FeaturesTrain1(Tn,:);
%% Calculating Euclidean distances
temp = norm(FeatureTest - FeatureTrain)^2;
Euc_dist = [Euc_dist temp];
end
[Euc_dist_min, Recognized_index] = min(Euc_dist);
```

As seen in this code the tested features distance calculated one by one with all trained features. Finally, the minum valu of this variable will give us the recognized index.

3.7 Other Methods

For comparision of the results, in this thesis three different methods are used and tested. These methods were local binary patter, principal component analysis and LoG Gabor.

3.7.1 Local binary pattern

The standard local binary pattern (LBP) operator for a pixel is a 3*3 window. This method works by comparing eight neighborhoods on the operator with the main pixel. Each of these eight neighboring pixels is replaced by 1 if its value is greater than or equal to the central pixel value, otherwise their value will be zero. At the end of the central pixel, it is replaced by the binary weighted addition of the neighboring pixels and the 3*3 window is moved to the next pixel. Taking a histogram of these values gives a descriptor for the texture of the image (Ojala et al. 2002).

Equation (3.17) shows the relation of local binary pattern formation in each pixel.

$$\mathrm{LBP}_{\mathrm{P,R}(x,y)} = \sum_{\mathrm{P}=0}^{\mathrm{P}-1} \mathrm{s}(\mathrm{g_p} - \mathrm{g_c}) 2^{\mathrm{P}} \tag{3.17}$$

where s represents the sign function, g_p and g_c are the values of the neighboring gray areas and the central pixel. Also, p 2 is the desired coefficient for each neighbor. The LBP architecture is shown in Figure 3.7.

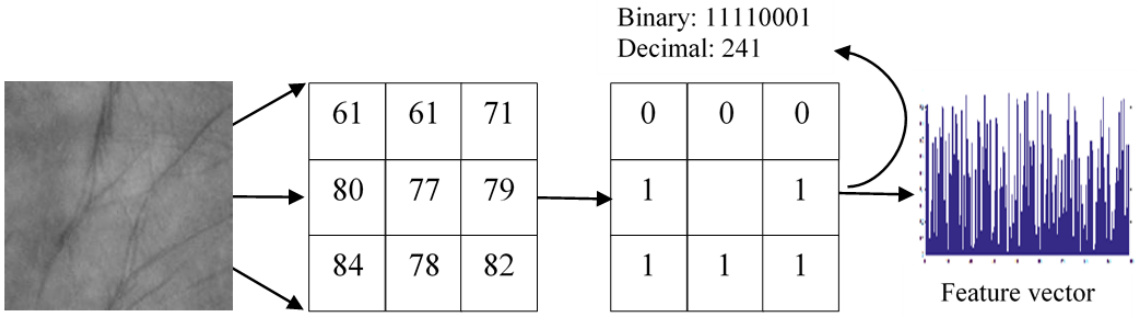

Figure 3.7 LBP architecture

As shown in the figure, by comparing each pixel with the central pixel in the 3 x 3 window, the code matrix is derived. We then multiply peer-to-peer code into the LBP operator. Finally, add the final numbers together to obtain the LBP label value (Liu et al. 2017).

Following the introduction of the standard LBP, the LBP method was extended to include tissues of different ratios, using neighbors of different sizes. Ojala and his colleagues (Ojala et al. 2002) developed their method of operating with circular neighbors with different radii. This operator is denoted as LBP(P, R), which denotes the number of neighbors on the circumference of a circle with radius R. Suppose that the central pixel C has coordinates (xc, yc), so the neighboring P pixel coordinates are expressed by Equations (3.18) and (3.19) where i = 1… P (Ojala et al. 2002).

$$x_i = x_c + Rcos\left(\frac{2\pi i}{P}\right) \tag{3.18}$$

$$y_i = y_c + Rsin\left(\frac{2\pi i}{P}\right) \tag{3.19}$$

Because of the use of sin and cos in the above formulas, the coordinates obtained may not be exactly on a single pixel, in which case the interpolation calculations of the gray area intensity of that point can be obtained.

Figure 3.8 shows an example of pixels calculated with radius and number of different neighborhoods.

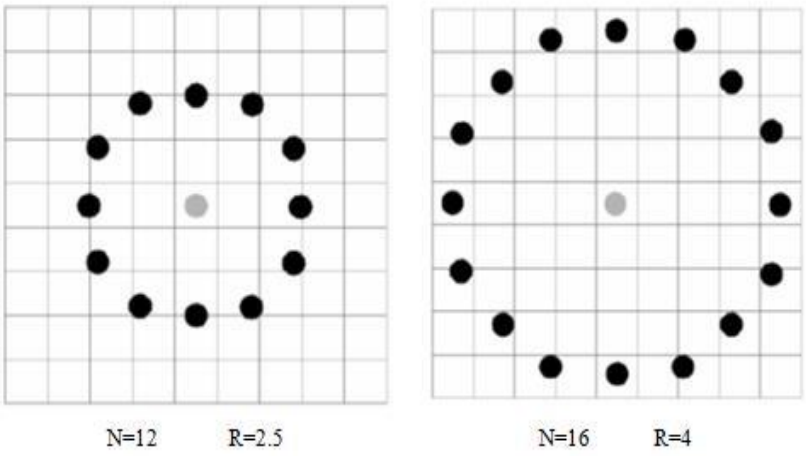

Figure 3.8 Locating the neighbors of an LBP operator in circles with different radius and neighborhood (Ojala et al. 2002)

These may be described by (P, R), where P is the number of interested pixels on the circle, while R is the radius of the used circle (Liu et al. 2017).

Figure 3.9 shows an example that divide the image to 8*8 blocks that these blocks has 8 pixels inside of them and the histogram result of this image.

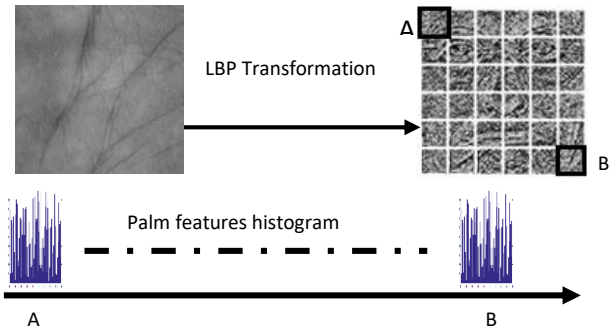

Figure 3.9 Applying the LBP on the image and getting the LBP features

3.7.2 Principle component analysis (PCA)

Principle component analysis (PCA) is a solution for mapping multidimensional data to a space with less dimension and less data loss. This method was proposed by Turk and

Pentland in 1991. The main idea of PCA is to reduce the size of the data in a data set so that changes in this data are maintained as much as possible. The basis of this method is that each image is treated as a point in an area with high dimensions. In the case of multiple images, these images are scattered dots in this high-dimensional space. Now we look for orthogonal vectors that by transferring data on those vectors, the data become as independent as possible. Therefore, this method looks for orthogonal vectors that meet this requirement as much as possible, and for this purpose, it uses principal element analysis, or PCA for short. In this method, first the data covariance matrix and then the matrix of vectors and eigenvalues are calculated. Matrices of special vectors are the orthogonal vectors that form the property subspace, and by transferring data to this subspace, the data becomes independent. To transfer data to this subspace, we multiply the data matrix in the matrix of special vectors or the new subspace vectors. Data transfer to this subspace has the important advantage that with this transfer, their volume is also reduced, which makes it possible to store information with a smaller volume, which is the case when the number and volume of data increases. Finds is of great importance. The special vectors used in this method for data transfer are orthogonal and are in the direction of maximum data scatter, and the expression of images in the new space is the expression of data with a minimum of squares error.

For the input image in this method, the image is first transmitted using a matrix of special vectors or vectors that make up the subspace. Then, in the reduced reduction space, it is compared with the available data and the most similar image is selected as the detected image. Criteria such as Euclidean, Manhattan, Cosine, etc. can be used for comparison. The new space that is created has dimensions equal to the dimensions of the image, and if the transfer vector is resized and displayed, images similar to the palm print image will be obtained. In fact, the goal is to express the input image using the linear coefficient of these images.

The advantages of this method include ease of implementation and use, reduction of data volume and high speed. Ignoring the dispersion within and between classes of data and not paying attention to the image tag to identify and differentiate between different images of a person in the database, is one of the disadvantages of this method, which

makes the maximum dispersion matrix, not only maximizes the scatter matrix between classes, which is useful for classification, but also maximizes the scatter matrix within classes, which is undesirable for classification. Also, the need to update all available information by entering a new image in the database is another disadvantage of this method. For this reason, the use of this method is more used as a dimensional method as preprocessing in other methods as neural networks. The mathematical calculations and steps of this method are as follows:

Convert an image matrix, which is a two-dimensional matrix, to a one-dimensional vector and put it together to form a data matrix. As a result, if we have a P image with dimensions r, c, the resulting data matrix will be a matrix with dimensions m * P, where m is the total number of pixels in the image, m = r * c.

• Calculate the average of the obtained matrix and transfer the data to center zero. To do this, after calculating the average image matrix, we subtract all images from the average matrix.

• Calculate the covariance matrix then its vectors and eigenvalues. In this step, we obtain the covariance matrix and calculate the matrix of special vectors and its eigenvalues.

• Transfer data matrix to new subspace using special vector matrices. To do this, we multiply the image vectors by the transfer vectors. By doing this, the original data, which are the same images, are converted into transferred data, which indicates the location of the data in the new vectors.

• Convert image matrices to vectors and move them to center zero. To do this, we subtract the input image from the average image of the original images.

• Transfer data vector to subspace using special vector matrices. To do this, like the operation for the original images, we multiply the new image vector by the transfer vectors.

• Check the similarity between the transferred vector and the existing vectors and select the most similar vector. To do this, based on the defined similarity criterion, we examine the image that most closely resembles the input image.

A theory in algebra states that two matrices and eigenvalues are the same, and that eigenvectors are equal to eigenvectors multiplied and normalized in the matrix. With the help of this theorem, special vectors can be obtained through the matrix, which is P * P, instead of calculating through the covariance matrix, which is N * N, because it has a lower computational load.

3.7.3 LoG

Log-Gabor (LoG) filter is a more sophisticated Gabor filter. Thus, before discussing Log-Gabor filters, a quick explanation of Gabor filters will be provided. In 1946, Dennis Gabor created the Gabor filter. When signals are in their best conjoint representation in the spatial and frequency domains, the filter provides the best representation of those signals.

Gaussian waves, sine waves, and cosine waves can all be combined to create Gabor filters. A singular conjoint localization in the frequency and spatial domains is produced by this method. These localizations are made in such a way that sine and cosine waves are very well localized in the frequency domain but are poorly localized in the spatial domain. In the spatial domain space, Gaussian simultaneously provides very good localisation. By combining sine and cosine waves with the Gaussian function, Gabor is able to provide accurate localisation in both the frequency and spatial domains.

After using Gabor, the decompression procedure creates two components (imaginary and real). The imaginary part is formed by sine/cosine waves, and the real part is produced by applying Gaussian. Figure 3.10 depicts the actual and fictitious components of a Gabor filter.

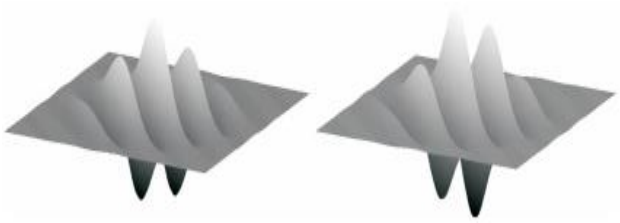

Figure 3.10 The real and imaginary part of Gabor

The terms even symmetric and odd symmetric are additional names for real and hypothetical parts. For the filter, the bandwidth and frequency center are defined. The bandwidth is defined by the gaussian width, and the frequency center is defined by the sine and cosine waves. The Gabor filter with two given dimensions (x, y) for an image is represented by the Equation (3.20).

$$G(x,y) = e^{-\Pi[(x-x_0)^2/a^2+(y-y_0)^2/\beta^2]}e^{-2\Pi[u_0(x-x_0)+v_0(y-y_0)]} \quad (3.20)$$

According to the formula above, (x_0, y_0) denotes the position of the pixels, (α, β) denotes the width and length of the Gaussain, and (μ_0, v_0) denotes the modulation with the spatial frequency $\omega 0 = \sqrt{\mu_0^2 + v_0^2}$.

3.8 Dataset

In this thesis, two famous datasets are used and tested. The first dataset was Polytechniques university of Taiwan that includes 500 people, and each person has 12 images. These images are gray level scale images with 227x227 image size. These images are captured by Canon camera that used in the university. The second dataset was Tongji Contactless dataset used by Zhang et al. (2017). Tongji dataset for contactless palmprints the Tongji Contactless Palmprint dataset is 12,000 pictures which are taken by a proprietary touchless acquisition method from 600 dissimilar palms. 192 men and 108 women who are the 300 participants that gave the photographs that Tongji University were using. They have included 235 individuals from the ages of 20 and 30 and the other individuals between the ages of 30 and 50. Two diffrent periods are used to collect the

left hand and right hand samples. 10 photos for each palm are provided in each session. For the result, each person provided 40 photos from both hands.

Researchers have given the hand biometric study a lot of attention, and it has resulted in an abundance of articles and technical reports. The Hong Kong Polytechnic University has been gathering contact-free 3D hand scans with the aim of creating a large-scale hand image database acquired using entirely contact-free imaging setup and making it freely available to the researchers in order to support the development of more user-friendly and reliable hand identification. There isn't yet a public database of contact-free 3D hand scans. To promote research efforts in the fields of hand geometry, 2D palmprint recognition, and 3D palmprint recognition, this collection contains textured 3D scans of the inside surface (palm-side) of the hand.

3.8.1 Description

The Minolta VIVID 910 3D digitizer, which is a readily available 3D digitizer, was used to capture the 3D hand images in the database. 177 respondents voluntarily provided their information for the database over the 4-month long data collection process. The participants were primarily our institute's students and staff, and they ranged in age from 18 to 50. They also came from a variety of ethnic backgrounds. In the first session, each participant gave 5 hand photos (range and a registered intensity image taken simultaneously), and in the second session, they each contributed an additional 5. Consequently, we presently have 3,540 hand photos in our database (of 3D and corresponding 2D). The interval between two data collecting sessions was not constant for all subjects; instead, it varied from one week at the least (for only 27 subjects) to three months at the maximum. The collection of all the hand photographs took place entirely indoors, with no limitations on the ambient lighting. In reality, our data collection technique was conducted at three different sites with noticeably variable ambient lighting. Every user is required to keep their right hand in front of the scanner during image acquisition at a distance of around 0.7 m, which was empirically determined to optimize the relative size of the hand in the acquired image frame. No restrictions were used to limit the posture of the hand, nor were the users told to take off any jewelry they were

wearing on their hands. However, in order to make the process of segmenting hands easier, a black background was made sure to be present behind the user's hand. Users were merely instructed to hold their hand inside the imaging area with the palm roughly parallel to the scanner's picture plane. By giving the consumers real-time visual feedback for hand positioning, this activity was made easier. Users were instructed to alter their hand position after each image was taken in order to add variants to the database. Every user's acquired images contain an integer identification/number that is used to consecutively number them. Both 3D and 2D, have a resolution of 640 × 480 pixels.

4. RESULTS AND DISCUSSION

4.1 Results

In this section the results of the proposed method are presetned. For first dataset total 500 people are used in the features extraction step. For feature extraction 80% of the data is selected as train data and 20% are selected as test data. In this study we didnt use any preprocessing or croption steps. Also, the frame of each images has 227x227 size. The dataset that contain of 500 people is shown in Figure 4.1.

With the exception of saving the feature sets in the database in MATLAB, the system does each process. The database is solely to be used for training. It is utilized in the system's evaluation component. The query image and the database's feature sets will be compared during the evaluation.

Following receipt of the feature set for the query image, the CNN procedure is carried out, during which the database images and the query picture is calculated. Calculated is the between the input image and images from other database classes. The aime of the CNN is to maximize relevance while minimizing redundancy. The classifying process is started after the CNN is determined.

After obtaining the features of train and test data matrix, the Euclidean distance between the query feature vector and the training feature vector is calculated for each class. The two matrices are subtracted to determine the Euclidean distance. The outcome also takes the shape of a matrix. The values of all squared values are then added after taking the square of each element. The square rooted is the outcome of the addition procedure. Euclidean distance is calculated in this manner. For six different classes, there will be six different Euclidean distance values.

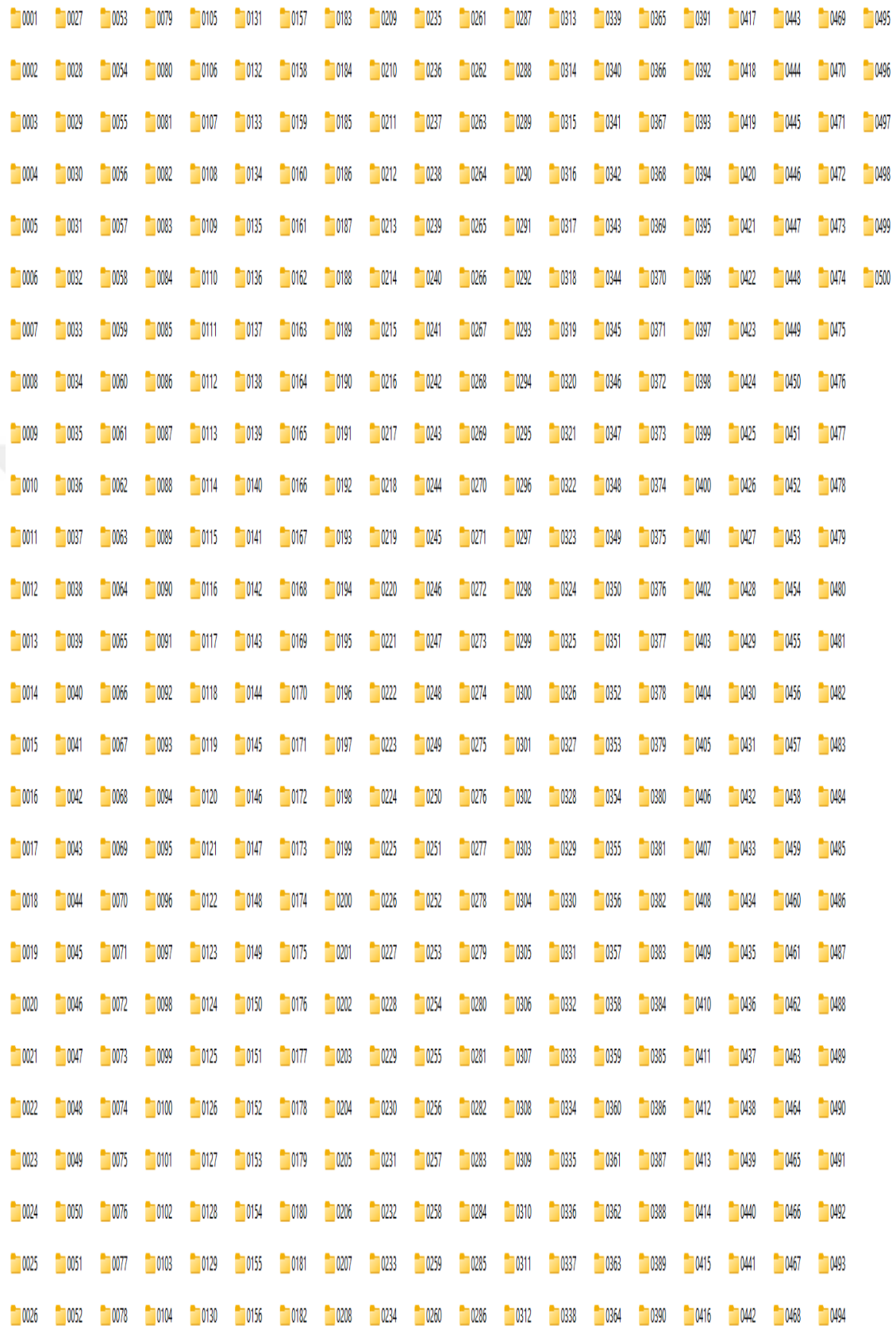

Figure 4.1 Dataset that contains 500 people

4.2 Results

The class to which the query image belongs will be determined by the minimum value of one of the six Euclidean distances. The following sample code show that how to use the Euclidian distance (see Figure 4.2).

```
for K = 1:size(FeaturesTest1,1)
    K
    FeatureTest = FeaturesTest1(K,:);
    Euc_dist = [];
    for Tn = 1:size(FeaturesTrain1,1)
        FeatureTrain = FeaturesTrain1(Tn,:);
        %% Calculating Euclidean distances
        temp = norm(FeatureTest - FeatureTrain)^2;
        Euc_dist = [Euc_dist temp];
    end
    [Euc_dist_min , Recognized_index] = min(Euc_dist);

    a = fix(Recognized_index/TrainNumber);
    b = mod(Recognized_index,TrainNumber);

    if a==0 || b>0
        a = a + 1;
    elseif b==0
        a = a;
    end
```

Figure 4.2 Sample code for the Euclidian Distance calculation

One image is being evaluated during the entire procedure. Numerous photos must be reviewed in order to gauge the system's effectiveness and accuracy. From all 500 persons images we selected the 2, 3, 4, 5, 6, 7, 8 test images seperatly and provided in the proposed method.

In this section, the results of simulations using MATLAB are shown. The experiment was performed using images that are taken from the dataset. The palm print recognition system consists of three stages. First of all, the images are recalled and split to train and test data. In the 2nd step the feature taken from images by using the pretrained network, also the other methods that are the triditional methods such as LBP, LoG, and Principle component analysing methods are used to extract the feature. These motheds are used

only to comparision of the results. In the last stage (recognition stage), the Euclidean distance is used as the recognition of the features. This method is tested on the Polytechnic Hong Kong dataset. The results are shown in Figure 4.3.

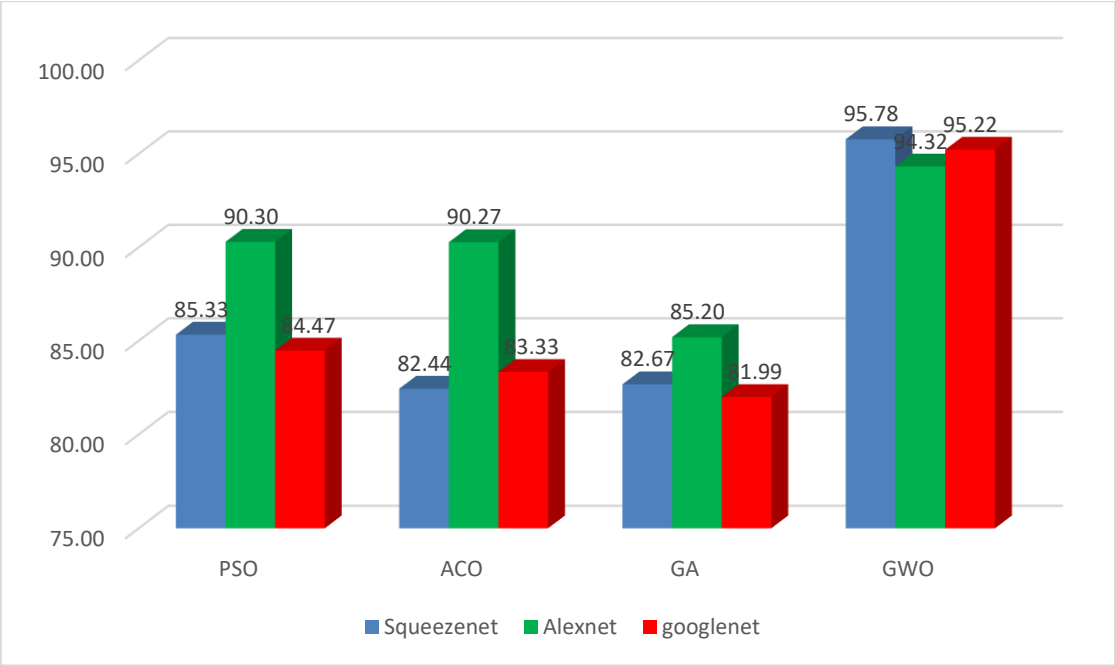

Figure 4.3 Recognition rates using proposed method versus of palm print state

The experiment was implemented to compare the performance of the palm print recognition system. This experiment was carried out with and without a preprocessing stage. The results obtained are summarized in Table 4.1.

Table 4.1 Results of proposed method with comparison other works

Reference	**Feature Extraction Method**	**Recognition Rate %**
Jamshidnezhad and Nordin (2011)	Geometric measurement	90.33%
Koelstra et al. (2010)	Quadtree Decomposition	94.30%
Yang et al. (2009)	Haar like feature	96.60%
Thai et al. (2011)	PCA	85.70%
Singh and Singh (2011)	Pattern Tracking	83.33%
Proposed method	**Deep Learning based on the GWO**	**96.23**%

4.3 Results and Analysis

The examination of the PER results is thoroughly covered in this section. To supporttraining and evaluation, two databases are employed. This thesis makes use of a database known as The Polytechnic Hong Kong database. The Tongji Contactless database is the name of the other database (Zhang et al. 2017). For seven different expressions, there are a total of 213 photos in the Polytechnic Hong Kong database. Typically, every application has a different ratio of the two sets. However, it is customary to retain the database's evaluation component at or above 70%. To lessen the degree of bias in the thesis, two separate sets are used. The system might be able to attain maximum accuracy if the photos from the training set were used for evaluation, but it might not be as efficient as if the same training set had been used. The system is assessed using a confusion matrix. In the classification experiment, performance is often evaluated using the confusion matrix. The diagonal of the matrix shows how well the dataset was recognized. The only values in the matrix that a classifier should use are those in the diagonal. The evaluations made by the machine utilizing the Polytechnic Hong Kong database are shown in Figure 4.4. The results from the Tongji Contactless database are shown in Figure 4.5. Accuracy in Figures 4.4 and 4.5 is calculated by Equation (4.1).

$$Accuracy = \frac{No.\ of\ correctly\ detected\ images}{Total\ No.\ of\ test\ images} \times 100 \quad (4.1)$$

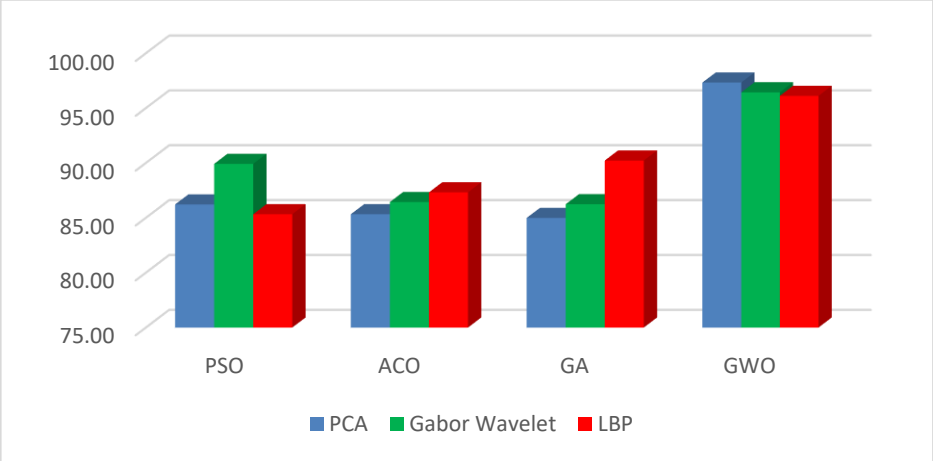

Figure 4.4 Accuracy chart for the Polytechnic Hong Kong database

The process time for Polytechnic Hong Kong dataset is shown in Figure 4.5.

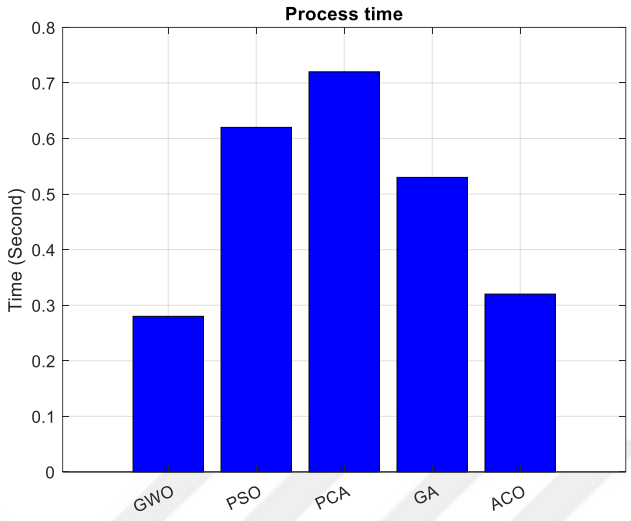

Figure 4.5 Process time for Polytechnic Hong Kong dataset

Figures 4.6 and 4.7 display the bar graphs for the accuracy levels reached for the Polytechnic Hong Kong database and the Tongji Contactless database, respectively. Figures 4.8 and 4.9 show accuracy along the horizontal and vertical axes, respectively.

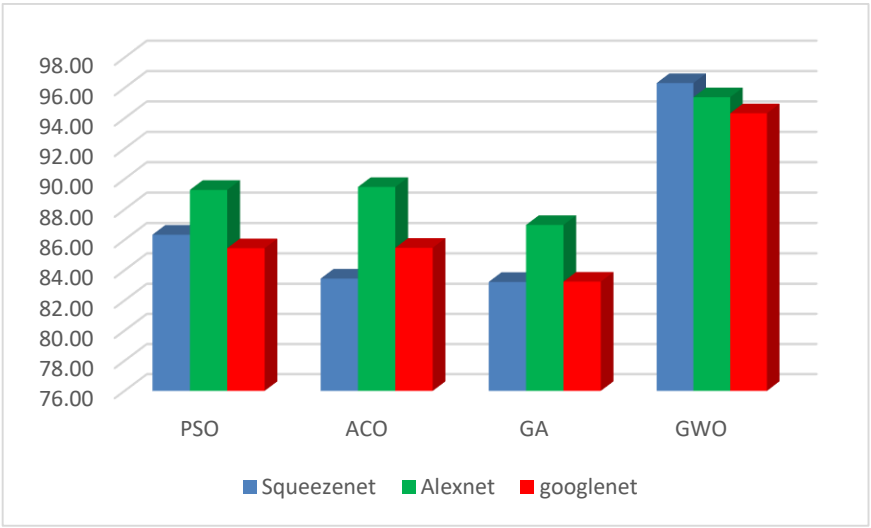

Figure 4.6 Accuracy chart for the Tongji Contactless Database

The process time for Tongji Contactless dataset is shown in Figure 4.7.

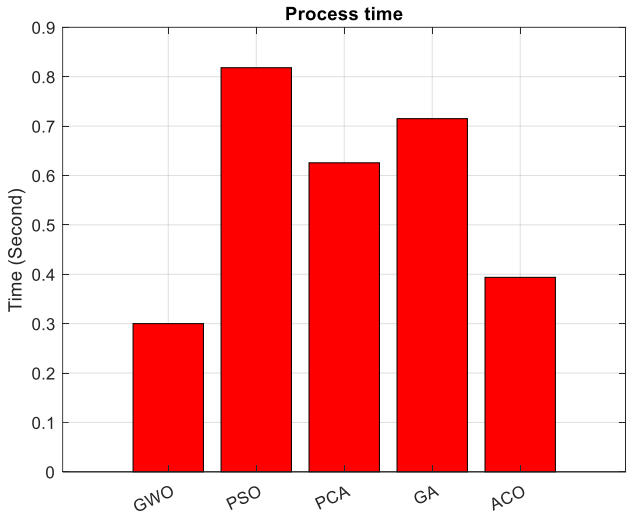

Figure 4.7 Process time for Tongji Contactless dataset

The experiment's incorrect predictions were made for a number of reasons. For each image, the training and evaluation sets use different illumination sources. Several photos also lack the palm prints in the middle. The palm print detector is forced to create smaller boxes for the palm print since they are near the ends of the frame rather than the middle. If only part of the palm print is photographed, it could interfere with the recognition process. As a result, the system becomes perplexed and forecasts inaccurate results. It is clear from looking through both databases that many subjects struggle to convey certain emotions, such as fear, rage, and disgust. As a result, it can be challenging to determine how the individual is feeling. No matter how accurate the classifier is, these issues prevent it from producing the desired results.

Every palm print that was found during the study is distinct in every photograph. Some subjects' palm impressions are larger, while others are smaller. The box that surrounds the palm print will therefore vary in size between images. The palm print may not always be completely removed from the photograph. The result would then differ from what was anticipated.

The PolyU database are used to evaluate the performance of the best feature extraction algorithm for palmprint recognition. To evaluate each algorithm, we looked into many

events and circumstances for this thesis. Principle Component Analysing (PCA), Local Binary Pattern (LBP), and Laplacian of Gaussian (LoG) Gabor are the four methods that have been compared using the MATLAB programming environment.

4.3.4 Experimental results

The experimental findings are divided into four categories. In the subsections that follow, the outcomes of each algorithm—PCA, LBP, and Log-Gabor—are illustrated.

Various experimental setups have been subjected to performance evaluation using PCA. For both the palmprint datasets, the number of train and test photos is raised from 150 to 470 images in each experiment set. The outcomes are shown in Table 4.2.

Table 4.2 Performance Evaluation (%) using PCA

Experiment Set	Number of Train Images	Number of Test Images	Recognition Rate (%)
1	285	367	95.67
2	443	392	96.04
3	404	388	92.21
4	457	276	95.44
5	360	360	95.24
6	161	205	91.30
7	422	376	90.95
8	449	160	93.99

The tables below show the PCA evaluation results for the right and palmprint datasets. Each class was given four photographs, two of which were utilized as training images and the other two as test images. The performance assessment for the hand is shown in Table 4.2, and the performance assessment for the hand is shown in Table 4.3. On the other hand, in the test set of PCA studies, different numbers of eigenvectors are chosen. The evaluation results for PCA with various eigenvector counts utilized in the technique are shown in Table 4.4.

Table 4.3 Performance of PCA with various eigenvector numbers for palmprint datasets

Number of Eigenvectors	Recognition Rate (%) Palmprint Dataset
100	66.81
150	68.32
200	70.23
250	71.68
300	72.56
350	74.00
400	74.90
450	74.90
469	74.90

Various experiments have been conducted to determine how LBP performance is evaluated. The tables below demonstrate many LBP experiments using the neighborhoods (1,8) and (2,16). Each person has two train images and two test images chosen from a total of four photos. Performance evaluation for and the hand in the area of (1,8) is shown in Table 4.4. (2,16). On cropped palmprint photos with a size of 150*150, we have conducted the experiments with a diversity of pattern sizes changing from 5*5 partitions to 13*13 partitions. For the palmprint datasets, respectively, Figure 4.8 show the results.

Table 4.4 Evaluation of LBP Performance for palmprint datasets

Pattern Size	Recognition Rate (%)	
	(1,8)	(2,16)
5X5	81.70	57.23
6X6	87.87	71.91
7X7	90.00	84.89
8X8	92.13	90.00
9X9	90.64	92.13
10X10	93.40	94.04
11X11	91.06	94.04
12X12	93.19	94.68
13X13	90.21	94.26

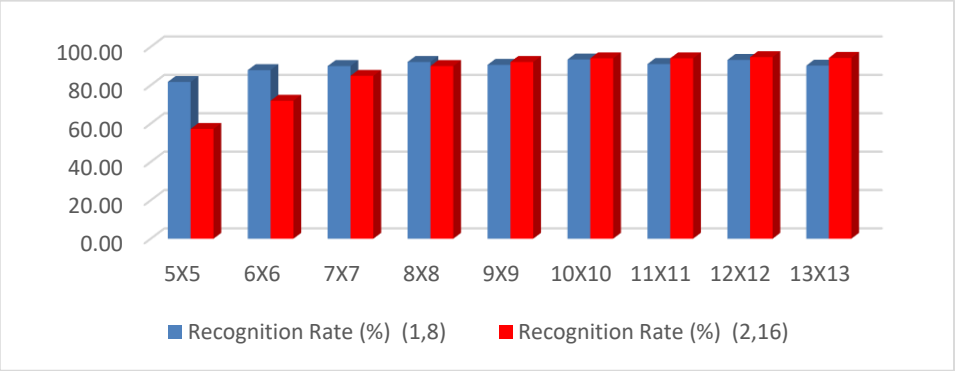

Figure 4.8 Performance evaluation of the Palmprint Dataset using LBP

235 classes have been used in the studies using the Log-Gabor technique on both the palmprint datasets. In these tests, two images were utilized for training and the remaining two were used for testing for the hand for each different class. The tables below demonstrate how altering the settings of the filter's parameter values affects performance. Each table shows the performance for various wavelength values and a certain sigma value. The palmprint datasets with various wavelength ranges ranging from 10 to 60 are used in the performance evaluation displayed in the following tables. The rates of palmprint identification are shown in Tables 4.5 using the respective sigma values of 0.45, 0.55, 0.6, and 0.65.

Table 4.5 Result for Log-Gabor

Experiment	Wavelength	Recognition Rate (%)
1	10	81.66
2	12	81.79
3	14	82.69
4	16	83.06
5	18	83.09
6	20	84.08
7	22	86.07
8	24	86.57
9	26	87.02
10	28	88.39
11	30	89.02
12	34	90.09
13	40	90.69
14	42	91.51
15	45	91.52

4.3.5 Discussion on experimental results

The effectiveness of palmprint recognition that uses Principal Component Analysis, Local Binary Patterns, and Log-Gabor changes when different parameter values are used for each approach. The simulations used two test shots and two training images, and the results showed that the Local Binary Patterns approach yields the best recognition performance.

The Local Binary Patterns method is offering the best recognition performance when comparing to other algorithms. The highest performance with LBP for the and hand is produced by the pattern size of 12*12 for the neighborhood of (2,16), which results in 94.6809% for the hand and 95.7447% for the left. Additionally, simulations noticied that the (1, 8) neighborhood consistently outperforms the (12 x 12) pattern size when the pattern size is 10 x 10. The accuracy for the hand (10*10) pattern size is 93.4043%, and the hand (91.4894%), whereas the accuracy for the hand (12*12) pattern size is 93.1915%, and the hand (92.5532%).

For instance, in the hand, when there are 470 samples in the dataset, 80.4255% can be produced. By lessing the number of trained and test samples in the dataset to 300 as the number of trained images and 300 as the number of test images, the performance increases to 78.3333%. When the ratio of train to test, images is getting down to 150, the performance increases to 80.6667%. The hand follows similar guidelines; when there are 470 trains and tests, the performance is 84.0426%. The performance increases to 85.6667% when the dataset is reduced to 300 train/test samples, while it reduces to 83.3333% when just 150 train/test samples are used.

However, Log-Gabor produced the third-best performance. The performance of this approach is highly dependent on the parameter values. As demonstrated in the preceding tables, the best palmprint recognition rate for the hand could be done when sigma is 0.45 and the wavelength is 40, which is 81.4894%. Similar to this, when sigma is 0.45 and the wavelength is 40, the hand employing Log-Gabor performs at its best. This condition's

palmprint identification rate is 80%, which is comparable to the results from the palmprint dataset.

In comparison to the other methods, PCA has the weakest recognition performance. For the hand, various experiments have been conducted. The best recognition rates utilizing the PCA technique were 74.6809% and 74.8926%, respectively, for palmprint datasets. Another set of PCA tests has been conducted to examine the identification rates for various eigenvector counts. When there are 380 eigenvectors, the hand performs best (75.7447%), and the hand performs best (74.8936%). Table 4.6 and Figure 4.9 provide a summary of the top recognition rates for each approach. For and palmprint datasets, a comparison of PCA, Log-Gabor, and LBP approaches is shown. The findings show that LBP achieves the highest identification rates in both left- and right-hand studies. The explanation for this is because LBP is a texture-based technique that highlights the most crucial characteristics and texture data present in palmprint photos.

Table 4.6 The most effective recognition rates for each method

Algorithm	Recognition rate (%) (palmprint datasets 1)	Recognition rate (%) (Palmprint datasets 2)
PCA	79.87	78.93
Log-Gabor	91.29	82.00
LBP	93.59	87.32

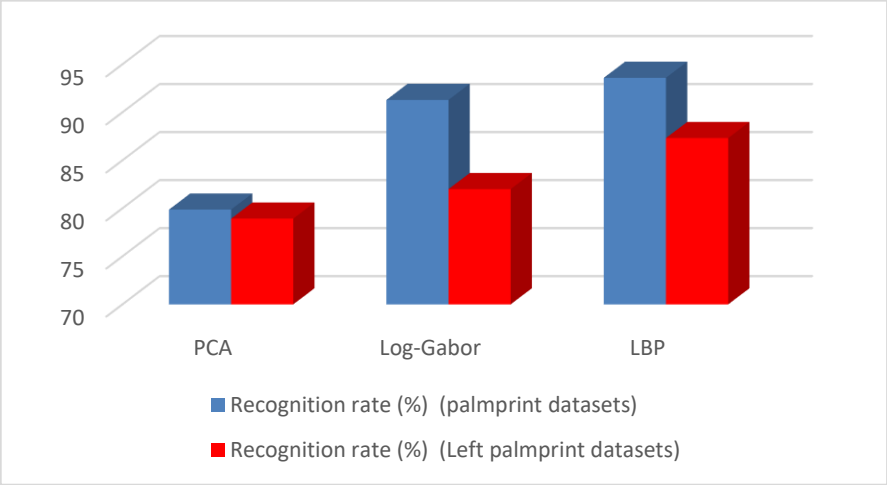

Figure 4.9 Comparison of four methods' performance

The deep learning model that used in this thesis is shown in Figure 4.10.

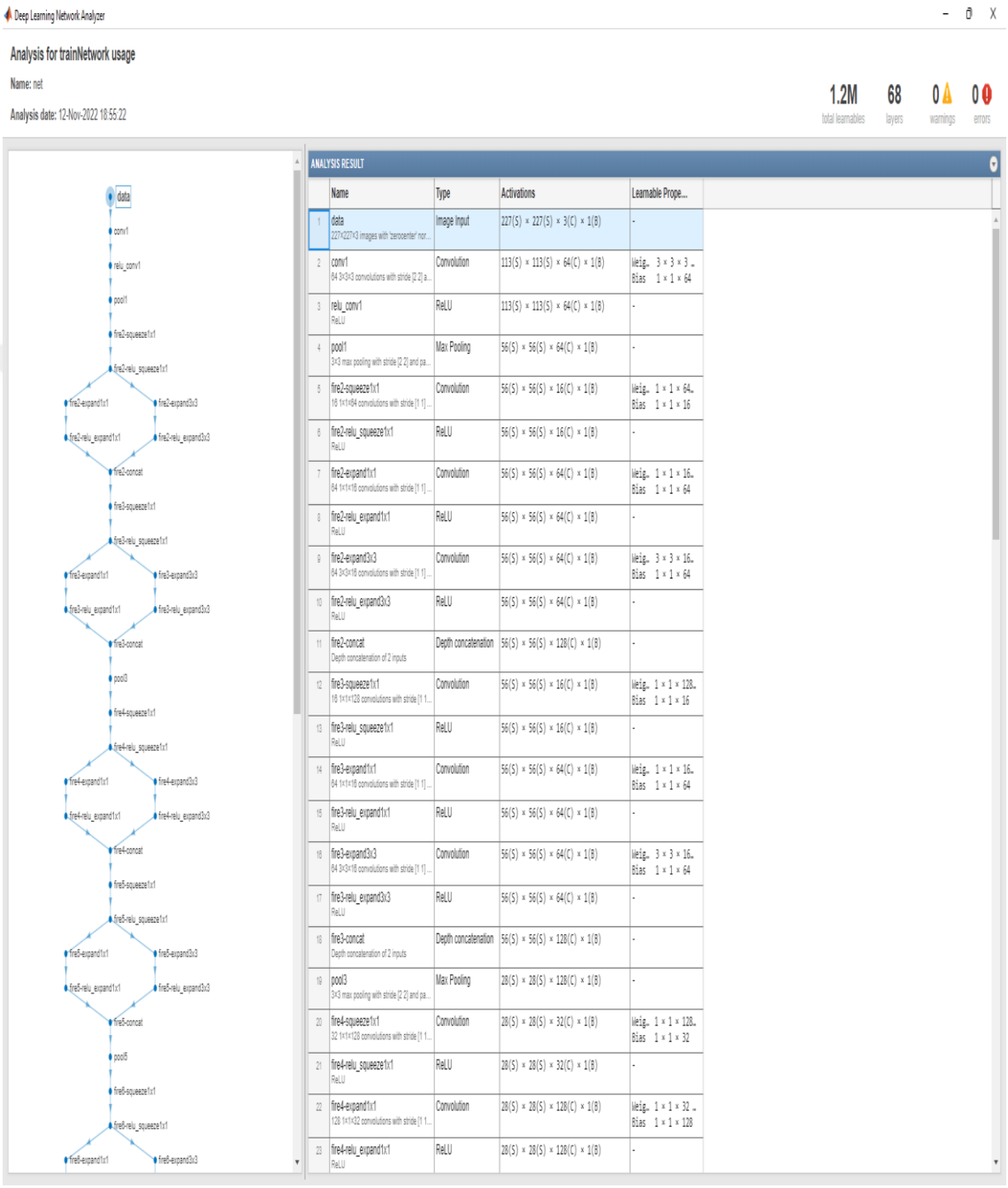

Figure 4.10 The DNN model

In this thesis, we used the squess network to extract the features. In this model 68 layers are used and this model is the pretrained model.

5. CONCLUSIONS AND FUTURE WORKS

Biometrics is an area of technology which uses a person's physical and behavioral traits tin order to identify them. Physical features include fingerprints, hand veins, palm lines, facial features, irises, and ears. Behavioral features include voice, hand movements and walking. Biometric authentication technology is palm recognition based on recognition of palm vein patterns using infrared, which is currently known as one of the most accurate biometric authentication solutions in today's era. Security systems to protect personal information, anti-theft devices for cars and vehicles, and anti-terrorist systems are used all over the world, relatively safe and low-risk security systems in various fields. Palm attendance devices provide a high level of accuracy. In this work, a palm identification system is implanted using the characteristics of blood veins that are located beneath the palm skin. The recognition of a person's personality based on their palm traits can can be measured from several angles, such as their vulnerability to the effects of aging and the environment, and they are thus considered as resistant to the same. The goal of the study was to develop an accurate palm identification system based on the aforementioned characteristics. The shape of the blood veins is determined by the structure of the palm surface (such as the shape of the main lifelines on the palm surface), making it distinct for each individual and potentially useful as a trait of identification.

In this thesis, for human identification we have used the palm print images. For feature extraction the deep learning and LBP methods are used. For reducing of the features, the Gray-Wolf optimization method is used. By using the GWO the best features are extracted. These features will be used in the deep learning for training of the dataset to be used in the test data. For evaluating the the results, the recognition rate percentage has been calculated. After checking the recognition rate with Euclidian distance method, the results are taked from this algorithm and calculated.

In future, we can use the deep learning with different scenario to train the system and use the trained networ to test the data. Also we can use the chameleon optimization, Crow search algorithm, and Bat algorithm to select the best features and use to train the deep learning.

REFERENCES

Abdoun, N., El Assad, S., Assaf, R., Déforges, O., Khalil, M. and Belghith, S. 2018. Design and implementation of robust Keyed Hash functions based on Chaotic Neural Network. Journal of Ambient Intelligence and Humanized Computing, 11(5): 2137-2161.

Adhinagara, Y., Agung, B. W. T. and Novi, D. R. 2011. Implementation of multimodal biometrics recognition system combined palm print and palm geometry features, In: Proceedings of the 2011 International Conference on Electrical Engineering and Informatics, pp. 1-5, Indonesia.

Alom, M. Z., Taha, T. M., Yakopcic, C., Westberg, S., Sidike, P., Nasrin, M. S., Van Esesn, B. C., Awwal, A. A. S. and Asari, V. K. 2018. The History Began from AlexNet: A Comprehensive Survey on Deep Learning Approaches. arXiv Prepr. arXiv1803.01164.

Attia, A., Mazaa, S., Akhtar, Z. and Chahir, Y. 2022. Deep learning-driven palmprint and finger knuckle pattern-based multimodal Person recognition system. Multimedia Tools and Applications, 81(8): 10961–10980.

Aykut, M. and Ekinci, M. 2013. AAM-based palm segmentation in unrestricted backgrounds and various postures for palmprint recognition. Pattern Recognition Letters, 34(9): 955–962.

Azman, A. R., Mahat, N. A., Wahab, R. A., Ahmad, W. A., Huri, M. A. M. and Hamzah, H. H. 2019. Relevant visualization technologies for latent fingerprints on wet objects and its challenges: a review. Egyptian Journal of Forensic Sciences, 9(1): 1–13.

Badrinath, G. S. and Gupta, P. 2012. Palmprint based recognition system using phase-difference information. Future Generation Computer Systems, 28(1): 287–305.

Balasubramanian, K. 2016. Cryptographic Solutions for Secure Online Banking and Commerce. IGI Global.

Bingöl, Ö. and Ekinci, M. 2017. Stereo-based palmprint recognition in various 3D postures. Expert Systems with Applications, 78: 74–88.

Chaa, M., Boukezzoula, N.-E. and Attia, A. 2017. Score-level fusion of two-dimensional and three-dimensional palmprint for personal recognition systems. Journal of Electronic Imaging, 26(1): 13018.

Dai, J. and Zhou, J. 2010. Multifeature-based high-resolution palmprint recognition. IEEE Transactions on Pattern Analysis and Machine Intelligence, 33(5): 945–957.

Fernández-Montoya, J., Avendaño, C. and Negredo, P. 2018. The glutamatergic system in primary somatosensory neurons and its involvement in sensory input-dependent plasticity. International Journal of Molecular Sciences, 19(1): 69-77.

Glorot, X. and Bengio, Y. 2010. Understanding the difficulty of training deep feedforward neural networks. In: Proceedings of the Thirteenth International Conference on Artificial Intelligence and Statistics, pp. 249–256, Italy.

Gopalakrishnan, K., Khaitan, S. K., Choudhary, A. and Agrawal, A. 2017. Deep convolutional neural networks with transfer learning for computer vision-based data-driven pavement distress detection. Construction and Building Materials, 157: 322–330.

Guo, Z., Zhang, D., Zhang, L. and Liu, W. 2012. Feature band selection for online multispectral palmprint recognition. IEEE Transactions on Information Forensics and Security, 7(3): 1094–1099.

Hammami, M., Ben Jemaa, S. and Ben-Abdallah, H. 2014. Selection of discriminative sub-regions for palmprint recognition. Multimedia Tools and Applications, 68(3): 1023–1050.

Hecht-Nielsen, R. 1992. Theory of the backpropagation neural network. In Neural networks for perception, pp. 65–93, Elsevier.

Jamshidnezhad, A. and Nordin, M. J. 2011. A classifier model based on the features quantitative analysis for facial expression recognition. International Journal on Advanced Science, Engineering and Information Technology, 1(4): 391–394.

Jia, W., Xia, W., Zhao, Y., Min, H. and Chen, Y. X. 2021. 2D and 3D palmprint and palm vein recognition based on neural architecture search. International Journal of Automation and Computing, 18(3): 377–409.

Jiaqiang, W., Ming, Y., Hanbing, Q. and Bin, L. 2013. Analysis of palm vein image quality and recognition with different distance. In: Fourth International Conference on Digital Manufacturing and Automation, pp. 215–218, China.

Kingma, D. P. and Ba, J. 2014. Adam: A method for stochastic optimization. ArXiv Preprint ArXiv:1412.6980.

Koelstra, S., Pantic, M. and Patras, I. 2010. A dynamic texture-based approach to recognition of facial actions and their temporal models. IEEE Transactions on Pattern Analysis and Machine Intelligence, 32(11): 1940–1954.

Konda, K. R. 2016. Unsupervised Relational Feature Learning for Vision. Ph.D. Thesis, Univ.-Bibliothek Frankfurt am Main, 152 page, Frankfurt.

Koonce, B. 2021. SqueezeNet, In: Convolutional Neural Networks with Swift for Tensorflow, Springer, pp. 73–85, New York.

Krizhevsky, A., Sutskever, I. and Hinton, G. E. 2017. ImageNet classification with deep convolutional neural networks. Communications of the ACM, 60(6): 84–90.

Liu, L., Fieguth, P., Guo, Y., Wang, X. and Pietikäinen, M. 2017. Local binary features for texture classification: Taxonomy and experimental study. Pattern Recognition, 62: 135–160.

Matheswaran, P., Navaneethan, C., Meenatchi, S., Ananthi, S., Janaki, K. and Manjunathan, A. 2021. Image Privacy in Social Network Using Invisible Watermarking Techniques. Annals of the Rom. Society for Cell Biology, 319–327.

Meraoumia, A., Chitroub, S. and Bouridane, A. 2011. Palmprint and Finger-Knuckle-Print for efficient person recognition based on Log-Gabor filter response. Analog Integrated Circuits and Signal Processing, 69(1): 17–27.

Miikkulainen, R., Liang, J., Meyerson, E., Rawal, A., Fink, D., Francon, O., Raju, B., Shahrzad, H., Navruzyan, A. and Duffy, N. 2019. Evolving deep neural networks, In: Artificial intelligence in the age of neural networks and brain computing. Elsevier, pp. 293–312, New York.

Mirjalili, S., Mirjalili, S. M. and Lewis, A. 2014. Grey wolf optimizer. Advances in Engineering Software, 69: 46–61.

Nguyen, B. P., Tay, W. L. and Chui, C. K. 2015. Robust biometric recognition from palm depth images for gloved hands. IEEE Transactions on Human-Machine Systems, 45(6): 799–804.

Nguyen, T. H. L., Arai, Y., Sato, H., Hayashi, T., Dong, F. and Hirota, K. 2008. A Speaker Recognition Method based on Personal Identification Voice and Trapezoid Fuzzy Similarity. SCIS and ISIS, 1596–1601.

Ni, J., Luo, J. and Liu, W. 2015. 3D palmprint recognition using Dempster-Shafer fusion theory. Journal of Sensors, 2015: 1-7.

Ojala, T., Pietikäinen, M. and Mäenpää, T. 2002. Multiresolution gray-scale and rotation invariant texture classification with local binary patterns. IEEE Transactions on Pattern Analysis and Machine Intelligence, 7: 971–987.

Raut, S. D., Humbe, V. T. and Mane, A. V. 2017. Development of biometrie palm vein trait based person recognition system: Palm vein biometrics system. In: 1st International Conference on Intelligent Systems and Information Management, pp. 18–21, Aurangabad, India.

Ravishankar, H., Sudhakar, P., Venkataramani, R., Thiruvenkadam, S., Annangi, P., Babu, N. and Vaidya, V. 2016. Understanding the mechanisms of deep transfer learning for medical images. In: Deep learning and data labeling for medical applications. Springer, pp. 188–196, USA.

Sato, T., Aoyama, S., Sakai, S., Yusa, S., Ito, K. and Aoki, T. 2013. A contactless palm recognition system using simple active 3D measurement with diffraction grating laser. In: 2nd IAPR Asian Conference on Pattern Recognition, pp. 542–546, Okinawa, Japan.

Schmidhuber, J. 2015. Deep learning in neural networks: An overview. Neural Networks, 61: 85–117.

Sethi, I. K. and Jain, A. K. 2014. Artificial neural networks and statistical pattern recognition: old and new connections. Elsevier, 286 page, USA.

Shin, H. C., Roth, H. R., Gao, M., Lu, L., Xu, Z., Nogues, I., Yao, J., Mollura, D. and Summers, R. M. 2016. Deep convolutional neural networks for computer-aided detection: CNN architectures, dataset characteristics and transfer learning. IEEE Transactions on Medical Imaging, 35(5): 1285–1298.

Singh, G. and Singh, B. 2011. Feature based method for human facial emotion detection using optical flow based analysis. An International Journal of Engineering Sciences, 4: 363–372.

Srivastava, N., Hinton, G., Krizhevsky, A., Sutskever, I. and Salakhutdinov, R. 2014. Dropout: a simple way to prevent neural networks from overfitting. The Journal of Machine Learning Research, 15(1): 1929–1958.

Szegedy, C., Vanhoucke, V., Ioffe, S., Shlens, J. and Wojna, Z. 2016. Rethinking the inception architecture for computer vision. In: Proceedings of the IEEE Conference on Computer Vision and Pattern Recognition, pp. 2818–2826, Las Vegas, USA.

Tan, C., Sun, F., Kong, T., Zhang, W., Yang, C. and Liu, C. 2018. A survey on deep transfer learning. In: International Conference on Artificial Neural Networks, pp. 270–279, Rhodes, Greece.

Thai, L. H., Nguyen, N. D. T. and Hai, T. S. 2011. A facial expression classification system integrating canny, principal component analysis and artificial neural network. ArXiv Preprint ArXiv:1111.4052.

Tiwari, K., Arya, D. K., Badrinath, G. S. and Gupta, P. 2013. Designing palmprint based recognition system using local structure tensor and force field transformation for human identification. Neurocomputing, 116: 222–230.

Torrey, L. and Shavlik, J. 2010. Transfer learning. In Handbook of research on machine learning applications and trends: algorithms, methods and techniques, pp. 242–264, IGI global.

Turčaník, M. 2017. Hash function generation based on neural networks and chaotic maps. 2017 Communication and Information Technologies, pp. 1–5.

Turčaník, M. and Javurek, M. 2016. Hash function generation by neural network. New Trends in Signal Processing, pp. 1–5.

Veigas, J. P. and Kumari M, S. 2022. Deep learning approach for Touchless Palmprint Recognition based on Alexnet and Fuzzy Support Vector Machine. International Journal of Electrical and Computer Engineering Systems, 13(7): 551–559.

Venkateswaran, R. 2001. Virtual private networks. IEEE Potentials, 20(1): 11–15.

Wang, J. G., Yau, W. Y., Suwandy, A. and Sung, E. 2008. Person recognition by fusing palmprint and palm vein images based on “Laplacianpalm” representation. Pattern Recognition, 41(5): 1514–1527.

Winn, J. K. 2022. Couriers without luggage: Negotiable instruments and digital signatures. In The Creation and Interpretation of Commercial Law, pp. 245–292, Routledge.

Wu, W., Elliott, S. J., Lin, S., Sun, S. and Tang, Y. 2020. Review of palm vein recognition. IET Biometrics, 9(1): 1–10.

Xin, Z. D. P., Xiaojing, G., Xiaoling, L. and Xin, P. 2015. Palmprint recognition based on deep learning. In Proc. 6th Int. Conf. Wireless, Mobile Multi-Media, pp. 214-216.

Xu, X., Guo, Z., Song, C. and Li, Y. 2012. Multispectral palmprint recognition using a quaternion matrix. Sensors, 12(4): 4633–4647.

Yang, B., Wang, X., Yao, J., Yang, X. and Zhu, W. 2013. Efficient local representations for three-dimensional palmprint recognition. Journal of Electronic Imaging, 22(4): 43040.

Yang, P., Liu, Q. and Metaxas, D. N. 2009. Boosting encoded dynamic features for facial expression recognition. Pattern Recognition Letters, 30(2): 132–139.

Yang, W., Wang, S., Sahri, N. M., Karie, N. M., Ahmed, M. and Valli, C. 2021. Biometrics for Internet-of-Things Security: A Review. Sensors, 21(18): 6163.

Yin, X., Yu, X., Sohn, K., Liu, X. and Chandraker, M. 2019. Feature transfer learning for face recognition with under-represented data. In: Proceedings of the IEEE/CVF Conference on Computer Vision and Pattern Recognition, pp. 5704–5713.

Yu, Y., Lin, H., Meng, J., Wei, X., Guo, H. and Zhao, Z. 2017. Deep transfer learning for modality classification of medical images. Information, 8(3): 91.

Yue, F., Zuo, W., Zhang, D. and Wang, K. 2009. Orientation selection using modified FCM for competitive code-based palmprint recognition. Pattern Recognition, 42(11): 2841–2849.

Zhang, D., Zuo, W. and Yue, F. 2012. A comparative study of palmprint recognition algorithms. ACM Computing Surveys (CSUR), 44(1): 1–37.

Zhang, L., Li, L., Yang, A., Shen, Y. and Yang, M. 2017. Towards contactless palmprint recognition: A novel device, a new benchmark and a collaborative representation based identification approach. Pattern Recognition, 69: 199–212.

Zhang, S. and Gu, X. 2013. Palmprint recognition method based on score level fusion. Optik-International Journal for Light and Electron Optics, 124(18): 3340–3344.

Zhao, K., Shen, L., Zhang, Y., Zhou, C., Wang, T., Zhang, R., Ding, S., Jia, W. and Shen, W. 2022. BézierPalm: A Free Lunch for Palmprint Recognition. In: European Conference on Computer Vision, pp. 19–36.

Zhong, D., Du, X. and Zhong, K. 2019. Decade progress of palmprint recognition: A brief survey. Neurocomputing, 328: 16–28.

CURRICULUM VITAE

Personal Information

Name and Surname : Firas Hasan Ali ALSHAKREE

Education

MSc	Çankırı Karatekin University Graduate School of Natural and Applied Sciences Department of Computer Engineering	2019-Present
Undergraduate	MOUSL University Faculty of Computer Sciences Department of Software Engineering	2005-2009